Glial ankyrins facilitate paranodal axoglial junction assembly

GLIAL ANKYRINS FACILITATE PARANODAL AXOGLIAL JUNCTION ASSEMBLY IN THE CENTRAL NERVOUS SYSTEM

Kae-Jiun Chang[1], Daniel R. Zollinger[2], Keiichiro Susuki[2], Diane L. Sherman[3], Peter J. Brophy[3], Edward C. Cooper[2,4], Vann Bennett[5], Peter J. Mohler[6] and Matthew N. Rasband[1,2]

[1]Program in Developmental Biology, [2]Department of Neuroscience, and [4]Department of Neurology, Baylor College of Medicine, Houston, TX 77030, USA, [3]Centre for Neuroregeneration, University of Edinburgh, Edinburgh, United Kingdom EH16 4SB, [5]Department of Cell Biology, Duke University, Durham, NC 27710, [6]Dorothy M. Davis Heart and Lung Research Institute, The Ohio State University, Columbus, OH 43210, USA.

Running title: Paranodal Ankyrins

*Correspondence should be addressed to:
Dr. Matthew N. Rasband
Department of Neuroscience
Baylor College of Medicine
One Baylor Plaza
Houston, Texas 77030

Tel: 713-798-4494
Fax: 713-798-3946
E-mail: rasband@bcm.edu

ABSTRACT

Neuron-glia interactions establish functional membrane domains along myelinated axons. These include nodes of Ranvier, paranodal axoglial junctions and juxtaparanodes. Paranodal junctions are the largest vertebrate junctional adhesion complex, are essential for rapid saltatory conduction, and contribute to assembly and maintenance of nodes. However, the molecular mechanisms underlying paranodal junction assembly are poorly understood. Ankyrins are cytoskeletal scaffolds traditionally associated with Na+ channel clustering in neurons and important for membrane domain establishment and maintenance in many cell types. Here, we show that ankyrinB, expressed by Schwann cells, and ankyrinG, expressed by oligodendrocytes, are highly enriched at the glial side of paranodal junctions where they interact with the essential glial junctional component neurofascin 155. Conditional knockout of ankyrins in oligodendrocytes disrupts paranodal junction assembly and delays nerve conduction during early development. Thus, glial ankyrins function as major scaffolds that facilitate early and efficient paranodal junction assembly in the developing central nervous system.

INTRODUCTION

Schwann cells in the peripheral nervous system (PNS) and oligodendrocytes in the central nervous system (CNS) wrap and insulate axons with myelin. They also actively cluster ion channels, cell adhesion molecules, and cytoskeletal scaffolds to form distinct functional domains along axons[1, 2]. For example, voltage-gated sodium (Nav) channels are highly enriched at nodes of Ranvier, while interactions between glial and axonal cell adhesion molecules (CAMs) flanking the nodes form paranodal junctions. Together, myelin, clustered ion channels, and paranodal junctions make action potential propagation much faster and more efficient.

Paranodal junctions perform several important tasks including: (1) restricting nodal proteins to assemble and maintain nodes; (2) separating juxtaparanodal voltage-gated K+ (Kv1) channels from nodal Nav channels; and (3) separating the periaxonal and extracellular spaces to fulfill myelin's insulating role [3-7]. An interacting set of CAMs, including axonal contactin and Caspr (contactin-associated protein) and glial NF155 (the 155-kDa isoform of neurofascin), are highly enriched at paranodes and are vital constituents of the junctions[1, 2]. Loss of any single paranodal CAM disrupts paranodal junctions, and causes delayed nerve conduction, tremor, and ataxia[8-10]. Despite their importance, the mechanisms regulating clustering and maintenance of paranodal CAMs

remain unknown.

Ankyrins have been implicated in formation and stabilization of membrane subdomains in many cell types[11, 12]. In the nervous system, ankyrinG (AnkG) is expressed by neurons and enriched at the axon initial segment (AIS) and node, where AnkG clusters Nav channels[13-16]. AnkyrinB (AnkB) is found in unmyelinated axons and regulates AIS assembly by establishing an intra-axonal boundary limiting the incorporation of AnkG into the distal axonal submembranous cytoskeleton[17, 18]. When axons are myelinated, in addition to nodal AnkG, AnkB and AnkG are detected at paranodes in the PNS and in the CNS, respectively [19-21]. Given the important roles of ankyrins in axon domain organization, we sought to determine if ankyrins contribute to the assembly and function of paranodes. Surprisingly, in contrast to previous reports, we found paranodal AnkB and AnkG are not axonal, but glial paranodal scaffolding proteins that interact with NF155. Furthermore, conditional knockout of ankyrins in oligodendrocytes disrupted paranodal junction formation and delayed nerve conduction during early CNS development. These results reveal a mechanism where glial paranodal ankyrins interact with NF155 to facilitate rapid paranodal junction assembly in the CNS.

RESULTS

Paranodal AnkB is in Schwann cells

The cytoskeletal scaffold AnkB is highly enriched at paranodal junctions in the PNS (**Fig. 1a**) and was previously reported to be in axons [19]. To determine if AnkB is important for paranodal junction assembly, we silenced AnkB expression in cultured dorsal root ganglion (DRG) neurons by using a highly efficient shRNA (short hairpin RNA) and GFP (green fluorescent protein)-expressing construct delivered by adenovirus[18]. AnkB protein expression was efficiently eliminated from GFP-labeled axons (**Fig. 1b**). However, after axons were myelinated by co-culturing with Schwann cells, most of the GFP-labeled axons still showed clear paranodal AnkB that accumulated at the edges of the myelin sheaths (**Fig. 1c**). One explanation for the remaining paranodal AnkB immunoreactivity is that a very small amount of residual AnkB may be sufficient to form paranodal clusters. Alternatively, paranodal AnkB may be in Schwann cells and unaffected by the shRNA in neurons. In support of the latter possibility we found that: (1) in some myelinated axons paranodal AnkB was located outside and surrounding the GFP-labeled axons (**Fig. 1d**), and (2) immunoblots comparing purified cultured Schwann cells with cultured hippocampal neurons showed low levels of AnkB in cultured Schwann cells (**Fig. 1e**). Furthermore, a transcriptome

analysis by Cahoy *et al.* reported a 2.1-fold increase in AnkB expression when comparing myelinating oligodendrocytes with oligodendrocyte precursors[22], suggesting that myelinating glia express AnkB. To clearly determine if paranodal AnkB is in axons or Schwann cells, we co-cultured AnkB-null[23] DRG neurons and wild-type Schwann cells, then induced myelination. If paranodal AnkB is in Schwann cells, it should be detected in this culture combination. Consistently, in the absence of axonal AnkB, we still observed paranodal AnkB (**Fig. 1f**). Together, these results show that AnkB is a glial component of paranodal junctions.

AnkB is not required for PNS paranodal junction assembly or function

To study the role of paranodal AnkB *in vivo*, we removed AnkB specifically from myelinating glia by crossing *Ank2-floxed* mice with *Cnp-Cre* mice [24] (*AnkB-cKO* or *Cnp-Cre;Ank2*$^{f/f}$; **Fig. 1g**); conventional AnkB knockout mice on a C57BL/6 background die at postnatal day (P) 0 before paranodal junctions form (data not shown). In *AnkB-cKO* sciatic nerves, AnkB staining was eliminated from paranodes (**Fig. 1h,i** arrows), consistent with the fact that paranodal AnkB is in Schwann cells and suggesting that neurons contribute no detectable AnkB to paranodal junctions. However, despite the strong enrichment of AnkB at paranodes in control mice, paranodal junctions, defined by

Caspr, NF155, and contactin, were assembled properly in *AnkB-cKO* mice (P28-P42 shown in **Fig. 1h,i** and **Fig. 2a,b**). In addition to their septate-like axoglial junctions, paranodes also have autotypic tight and adherens junctions between adjacent cytoplasmic loops[2]. In the *AnkB-cKO* mice, paranodal tight junctions (**Fig. 2c**), adherens junctions (data not shown) and the distribution of other paranodal loop components (**Fig. 2d-g**) were all unaffected, indicating AnkB is not essential for the overall architecture of PNS paranodes.

Paranodal junctions act as diffusion barriers that separate juxtaparanodal proteins from nodal proteins. Although the axonal paranodal scaffolds 4.1B and βII spectrin are not required for paranodal junction formation, they are crucial for barrier function[25-27]. To determine if paranodal AnkB plays a similar role in regulating juxtaparanodal protein localization from the glial side, we analyzed the distribution of Kv1.2 and Caspr2 in *AnkB-cKO* mice. We found that AnkB played no essential role in regulating juxtaparanodal protein localization (**Fig. 2h,i**). Consistent with the normal localization of nodal, paranodal, and juxtaparanodal proteins we also measured no significant delay in nerve conduction velocities along the *AnkB-cKO* sciatic nerves compared to control nerves (**Fig. 2j**).

We considered the possibility that loss of AnkB could delay paranode formation, or

result in eventual paranode degeneration and loss of polarized axon domains in aged mice. However, we found that paranodal junctions formed normally in P3 sciatic nerves (**Fig. 2k**), and one-year-old *AnkB-cKO* mice had normal paranodes and juxtaparanodal clustering of Caspr2 (**Fig. 2l**). Finally, paranodal junctions have previously been implicated in switching of nodal Nav channel subtypes from Nav1.2 to Nav1.6 during development, since mice with disrupted paranodal junctions retain Nav1.2 at nodes[6, 28]. However, nodes in *AnkB-cKO* mice had Nav1.6 but no Nav1.2 (**Fig. 2m**), indicating that AnkB is not involved in the signaling pathway that regulates Nav channel subtype expression. Together, these results demonstrate that AnkB is a glial paranodal protein, but surprisingly is not required for paranodal junction formation, function, or maintenance.

AnkG is clustered at the glial side of CNS paranodes

Immunostaining of the dorsal root entry zone from P31 mice showed that AnkG is enriched at nodes and CNS paranodes (**Fig. 3a,** arrow), while AnkB is found at PNS paranodes; we rarely observed AnkB at CNS paranodes (**Fig. 3a**)[19]. Although AnkG has been strongly implicated in Nav channel clustering at nodes[14, 16], the role and cellular source of paranodal AnkG are unknown. Since paranodal AnkB is made by Schwann

cells in the PNS, and since AnkG is 5.7 times more enriched in oligodendrocytes compared to neurons and astrocytes[22], we wondered if paranodal AnkG is also found in myelinating oligodendrocytes where it could contribute to paranodal junction assembly. To test this possibility, we constructed AnkG-deficient oligodendrocytes by crossing *Ank3-floxed* mice with *Cnp-Cre* mice (*AnkG-cKO* or *Cnp-Cre;Ank3$^{f/f}$*; **Fig. 3b**). Control mouse optic nerves showed both nodal and paranodal AnkG immunoreactivity (**Fig. 3c,d**). However, *AnkG-cKO* mice had only nodal AnkG (**Fig. 3e**), indicating that paranodal AnkG is found in oligodendrocytes. Thus, myelinating Schwann cells have paranodal AnkB, while myelinating oligodendrocytes have paranodal AnkG.

AnkG is required for CNS paranodal junction assembly during early development

To determine if paranodes require AnkG for normal function, we examined their assembly during myelination in *AnkG-cKO* mice. Prior to the formation of full nodes (defined here as nodal clusters of βIV spectrin flanked by Caspr-labeled paranodal junctions on both sides), three kinds of nodal intermediates can be observed: 1) paranodes only, 2) nodes alone without flanking paranodal junctions, and 3) heminodes with paranodal junctions only on one side[5, 20](**Fig. 3h**). We found in the optic nerves of P12 wild-type (WT) mice that the majority of nodal βIV spectrin clusters are flanked by

one or two Caspr-labeled paranodes (only 16.7±1.6% were lacking paranodal Caspr; **Fig. 3f,h**). In sharp contrast, the majority (53.5±0.9%) of nodal βIV spectrin clusters in *AnkG-cKO* optic nerves lacked flanking paranodal Caspr (**Fig. 3g,** arrows, and **h**). This defect in paranodal junction assembly was further reflected in a significant delay in the conduction velocity of compound action potentials (CAPs) in P17 *AnkG-cKO* optic nerves (**Fig. 3i,j**). Thus, oligodendrocyte AnkG is required for normal paranodal junction assembly and function.

Although we found a severe defect in paranodal junction assembly in the *AnkG-cKO* at P12, many paranodal junctions were still observed (**Fig. 3h**). Since AnkG contributes to both assembly and maintenance of axon initial segments [29-32], we speculated that these AnkG-independent paranodal junctions might degenerate in older *AnkG-cKO* mice. However, a detailed analysis of nodes and nodal intermediates in P12-P56 *AnkG-cKO* optic nerves revealed that the number of paranodal junctions actually approached WT levels by P56. Furthermore, we measured no delay in the CAP conduction velocity along P56 *AnkG-cKO* optic nerves compared to WT mice (data not shown), and juxtaparanodal clustering of Kv1 channels was normal in P22 (**Fig. 4b**) and 1-year old *AnkG-cKO* mice (**Fig. 4c**). Together, these results suggest that paranodal junctions are assembled less efficiently in the absence of paranodal AnkG, but that they

eventually recover and do not require AnkG for their maintenance.

AnkB partially compensates for the loss of AnkG at CNS paranodes

The gradual recovery of paranodal junction formation suggests that other mechanisms or molecules may compensate for the loss of AnkG. To determine if other ankyrins compensate, we examined the expression of the two other vertebrate ankyrins: AnkR and AnkB. Although we observed no AnkR at paranodes (data not shown), we did find many more AnkB-enriched paranodes in the *AnkG-cKO* optic nerves (**Fig. 4d,e**), suggesting AnkB may substitute for AnkG and rescue paranodal junction assembly in *AnkG-cKO* mice. To test this possibility, we constructed *AnkB/AnkG* double cKO mice (*AnkB/G-cKO*) using *Cnp-Cre* to remove AnkB and AnkG from oligodendrocytes. *AnkB-cKO* mice showed virtually no defects in paranodal junctions in the CNS (**Fig. 4a,f**). In contrast, when compared to *AnkG-cKO* mice, *AnkB/G-cKO* mice showed more severe defects in paranodal junction assembly throughout development, (**Fig. 4a,g**), and they also had slower nerve conduction velocities (**Fig. 3j**). Thus, AnkB can partially compensate for the loss of AnkG in oligodendrocytes. Nevertheless, paranodal junctions still formed in the *AnkB/G-cKO* mice, and the differences between the *AnkB/G-cKO*, *AnkG-cKO*, and WT mice became smaller with increasing age (**Fig. 4a**).

Since myelination is a prerequisite for formation of nodes and paranodal junctions, one possible explanation for the paranodal changes described here is that myelination is delayed in the absence of glial ankyrins, and defective paranodal junction formation is secondary to delayed myelination. Importantly, we found that the density of nodal βIV spectrin clusters was similar among the WT, *AnkG-cKO*, *AnkB-cKO*, and *AnkB/G-cKO* mice (data not shown). Furthermore, electron microscopy of P17 WT and *AnkB/G-cKO* optic nerves showed no difference in the number or percentage of myelinated axons (**Fig. 4j-l**). These results indicate that myelination and paranodal junction assembly proceeds in the absence of paranodal ankyrins, but proper paranode formation occurs at a much reduced rate.

AnkB and AnkG interact with NF155

To understand the molecular mechanism whereby AnkG and AnkB regulate rapid paranodal junction assembly, we sought to identify their paranodal membrane protein binding partner. One possibility is that paranodal ankyrins function in concert with NF155, since NF155 is an essential component of paranodal junctions, and ankyrins bind to the cytoplasmic domain of neurofascins [33, 34]. To test this possibility, we closely examined NF155 and AnkB localization in developing sciatic nerves. We found that

NF155 tended to be more enriched in subregions of paranodes where AnkB was located (**Fig. 5a,b**). Furthermore, when AnkB extended beyond Caspr, NF155 extended together with AnkB (**Fig. 5c,d**), suggesting that during early development NF155 localization is more closely aligned with AnkB than with Caspr. Although paranodal NF155 was previously reported to be phosphorylated[35] (which should block its interaction with ankyrins[33, 34]), immunoreprecipitation of AnkB from sciatic nerve and AnkG from spinal cord, in the presence of phosphatase inhibitors, co-precipitated NF155 (**Fig. 5e,f**). Taken together, these results suggest that some paranodal NF155 is not phosphorylated and interacts with paranodal ankyrins *in vivo*.

We previously proposed that during myelination, the initial interaction between glial NF155 and axonal Caspr/contactin assembles a paranodal lipid microdomain that promotes recruitment and stabilization of additional NF155 and Caspr/contactin molecules[36]. To determine if ankyrins contribute to these early events, we asked if they are recruited by NF155 to paranodal junctions. In *Caspr-KO* mice, paranodal junctions do not form and most paranodes have no detectable NF155 or AnkB (**Fig. 5g, h**)[8]. However, at some paranodes, low levels of colocalized AnkB and NF155 could still be detected (**Fig. 5i,** arrows). A similar but more prevalent phenomenon of paranodal, colocalized AnkG and NF155 was also seen in the *Caspr-KO* spinal cord (**Fig. 5j,** and **k,**

arrows). These observations suggest targeting of AnkB and AnkG to paranodes does not require intact paranodal junctions, and argues against the idea that ankyrins are passively recruited by NF155/Caspr/contactin junctional complexes. In further support of this idea, we analyzed sciatic nerve paranodal junctions from *Nfasc-KO* mice transgenically rescued using an NF155 construct that lacks its intracellular ankyrin-binding motif (NF155ΔIC)[37]. In some cases paranodal AnkB could be clearly observed (**Figs. 5l-n,** arrows). These observations suggest that ankyrins can be targeted to paranodes independently of NF155.

Schwann cells and oligodendrocytes express 220-kDa AnkB from multiple promoters

Previous studies have reported a variety of different ankyrin splice variants in the nervous system. For example, neurons express both 270- and 480-kDa isoforms of AnkG at the AIS and nodes[13], and 440-kDa AnkB is expressed in unmyelinated axons[17, 38]. To determine if distinct isoforms of AnkB and AnkG are utilized by glia at paranodal junctions and how different cell types regulate expression of AnkB and AnkG, we designed isoform-specific primers and performed quantitative reverse transcription-polymerase chain reaction (qRT-PCR) analysis on P31 sciatic nerves and

spinal cords to detect the levels of various transcripts of AnkB and AnkG, respectively. Alternative splicing of the 6.2-kb giant exon of *Ank2* (exon 40) can produce two AnkB isoforms: a 220-kDa AnkB produced by exclusion of exon 40, and a 440-kDa giant AnkB by inclusion of exon 40[11] (**Fig. 6e**). Exon 24 is removed by our conditional knockout strategy (**Fig. 1g**), and we detected a graded reduction in the exon 24-containing transcripts in the *AnkB-cHet* and *AnkB-cKO* sciatic nerves and spinal cords (**Fig. 6a, d**). Similarly, we observed a graded decrease in the levels of the transcripts without exon 40 (220 in **Fig. 6a, d**) but no significant decrease in the transcripts with exon 40 (440 in **Fig. 6a, d**). Consistently, Western blotting of sciatic nerves and spinal cord homogenates showed a dramatic reduction of 220-kDa isoform of AnkB in the *AnkB-cKO* (**Fig. 6b, c**). These results suggest Schwann cells and oligodendrocytes express the 220-kDa AnkB.

According to one previous study[39] and the current Ensembl database, there are five alternative promoters available to express AnkB. We designated the first exons driven by these promoters as exon 1'', exon 1' (exon 0 in [39]), exon 1, exon '1 and exon 1s from upstream to downstream (**Fig. 6e; Supplementary Table 1**). To determine which first exon of AnkB is used by myelinating glia, we performed qRT-PCR to measure transcript levels; in our analysis we excluded exon 1s because antibodies specifically against AnkB's spectrin-binding and C-terminal tail domain did not label paranodes in *AnkB-cKO*

mice (data not shown). We found that myelinating glia in sciatic nerves and spinal cords use multiple promoters: Schwann cells mainly express exons 1- and ‘1-containing transcripts, while oligodendrocytes express exons 1’ and ‘1-containing transcripts of AnkB (**Fig. 6a, d**).

Oligodendrocytes express 190-kDa and 270-kDa AnkG isoforms by using the promoter at exon 1b

AnkG also undergoes extensive alternative splicing[11]. Its splice variants include 480-, 270-, and 190-kDa isoforms depending on whether and how the giant exon is incorporated (exon 41 in **Fig. 7f**). To reveal the isoforms expressed by oligodendrocytes, we performed qRT-PCR analysis of AnkG splicing on P31 spinal cords. Since exon 23 is removed by our conditional knockout strategy (**Fig. 3b**), we observed a graded decrease in exon 23-containing transcripts in the *AnkG-cHet* and *AnkG-cKO* (**Fig. 7a**). Among all the AnkG isoforms analyzed, the 190-kDa isoform-encoding transcripts showed the largest decrease, suggesting the majority of the 190-kDa isoform transcripts in P31 spinal cords are expressed by oligodendrocytes. Although the AIS and nodal 480-kDa isoform remained unchanged in the *AnkG-cHet* and *AnkG-cKO*, surprisingly the 270-kDa isoform also exhibited a graded decrease similar to that detected in exon 23, suggesting

that it is expressed by both neurons and oligodendrocytes. Therefore, we examined the localization of the 270-kDa isoform using antibodies specific for 480/270-kDa AnkG[13]. Consistent with our qRT-PCR results, the anti-480/270-kDa AnkG antibody stained both nodes and paranodes in WT mice (**Fig. 7c**), but failed to stain paranodes in *AnkG-cKO* mice. Immunoblots of spinal cord homogenates also showed decreases in the 190- and 270-kDa isoforms in the *AnkG-cKO* mice (**Fig. 7b**). Thus, oligodendrocytes express both 190- and 270-kDa AnkG.

Five alternative first exons have been identified for AnkG: 1a, 1b, 1e, 1f and 1s[31, 40] (1a, 1b, 1e and 1s correspond to I, III, 1 and 23, respectively in [41]; **Supplementary Table 2**). Because exon 1s is located between exons 25 and 26, exon 1s-containing AnkG should not be affected by our conditional knockout strategy (**Fig. 7f** and **3b**). However, since our strategy eliminated paranodal AnkG, exon 1s-containing AnkG cannot be utilized by oligodendrocytes at paranodal junctions. To identify the AnkG promoter used by oligodendrocytes, we first stained spinal cord sections with antibodies against unique peptide sequences encoded by exons 1b and 1e[31]. We found that nodal AnkG includes exon 1b- and 1e-containing AnkG proteins, whereas oligodendrocytes only have exon 1b-containing AnkG at paranodes (**Fig. 7d**). To determine if exon 1a or 1f is also used by oligodendrocytes, we analyzed paranodal AnkG in the conventional KO of *Ank3* exon 1b,

which is considered to be a cerebellum-specific KO[31]. Interestingly, paranodal AnkG was absent from the exon 1b KO (**Fig. 7e**), indicating that exon 1b is the main exon 1 utilized by oligodendrocytes and that the exon 1b KO is also a KO that affects oligodendrocytes. Consistent with these results, exon 1b-containing transcripts also showed a graded reduction in *AnkG-cHet* and *AnkG-cKO* mice (**Fig. 7a**). (The levels of exon 1e-containing transcripts decreased in the *AnkG-cHet*, but there was no significant further reduction detected in the *AnkG-cKO* suggesting this is likely an effect of heterozygosity in *Cnp*; the *Cnp-Cre* allele is simultaneously a Cre knock-in and *Cnp* KO allele[24]). Thus, oligodendrocytes express 190-kDa and 270-kDa AnkG from the promoter at exon 1b. Our discovery of glial ankyrins and their alternative splicing compared to neuronal ankyrins reveal another level of complexity in neuron-glia interactions that parallels the situation for neurofascins: neurons express NF186 at the AIS and node, whereas myelinating glia express NF155 at paranodal junctions[37, 42, 43]. Thus, the same genes, but different splice variants, can be used by both neurons and myelinating glia for different functions.

DISCUSSION

Ankyrins organize membrane subdomains in diverse cell types and regulate cell-cell interactions through these domains[11, 12]. The ankyrin and spectrin-based cytoskeleton also provides cells with membrane flexibility and toughness. For example, without functional AnkR, the plasma membranes of red blood cells become fragile, resulting in spherocytosis and anemia. In the nervous system, ankyrins and spectrins are reiteratively used to assemble polarized subdomains and support the delicate structure of axons and myelin[18, 44-47]. Ankyrins were previously identified at paranodes[19, 20], but their cellular source and functions remained unknown. Here, we showed that paranodal AnkB is produced by Schwann cells. However, this AnkB is dispensable for paranodal junction formation, function, and the organization of axonal membrane domains. In the CNS, AnkB is seldom observed at paranodes. Instead, AnkG is enriched at both paranodes in oligodendrocytes as well as in axons at nodes of Ranvier. Furthermore, the selective deletion of AnkG from myelinating glia caused a severe defect in paranodal junction formation during early development (**Supplementary Fig. 1**).

Our data show that paranodal ankyrins interact with NF155 *in vivo* to regulate the early phase of CNS paranodal junction assembly. The interaction between neurofascin and ankyrins is required for aggregation of neuroblastoma cells mediated by homophilic

neurofascin interactions [34]. Disruption of neurofascin's cytoplasmic interaction with ankyrins increases its lateral mobility and severely compromises the ability of neurofascin-expressing cells to form large aggregates[33, 34]. Based on the multivalent binding property of ankyrins with more than one neurofascin molecule and two ankyrin-binding sites on one spectrin tetramer (which links the neurofascin-ankyrin protein complex to the actin cytoskeleton), we speculate that interactions between NF155 and ankyrins may stabilize many paranodal NF155 molecules in close proximity to one another to increase binding avidity for axonal Caspr/contactin.

Why do paranodal ankyrins play more important roles in the CNS than the PNS? In the CNS, paranodal junctions function as lateral diffusion barriers and are the primary mechanism responsible for clustering of AnkG, Nav channels, and βIV spectrin at nodes of Ranvier[5]. In contrast, paranodal junction formation in the PNS follows clustering of nodal proteins and plays a secondary role to that of heminodal clustering by gliomedin[4, 48] (**Supplementary Fig. 1b**). This contrast may be partially explained by the observation that NF155 is expressed by oligodendrocytes before myelination, whereas Schwann cells express NF155 only after the onset of myelination and the initiation of nodal protein clustering[36, 43, 49]. Similarly, paranodal clustering of ankyrins is detected during early myelination in the CNS[20], but only after Caspr clustering in the PNS[19]. Our results also

suggest paranodal targeting of ankyrins does not require paranodal junctions or NF155. Based on these observations, we propose that during early CNS myelination, ankyrins facilitate the accumulation of NF155/Caspr/contactin clusters by actively targeting NF155 to paranodes, or by clustering and stabilizing the earliest NF155/Caspr/contactin complexes at paranodes. Without paranodal ankyrins in the CNS, paranodal junction formation is severely delayed and preceded by nodal clustering, similar to the normal situation in the PNS (**Supplementary Fig. 1b**). To further understand the molecular mechanisms by which ankyrins facilitate paranodal junction assembly, it will be important to determine the paranodal targeting mechanisms for AnkB and AnkG. Intriguingly, myelin compaction seems to be a prerequisite for paranodal targeting of AnkG[20].

Although we observed a significant delay in CNS paranodal junction formation, our results show paranodal ankyrins are not absolutely required for junction assembly in the PNS or CNS. The eventual formation of paranodal junctions is not due to compensation by other ankyrins since neither AnkG nor AnkR compensate for the loss of AnkB in the PNS, and AnkR does not compensate for the loss of both AnkG and AnkB in the CNS (data not shown). We speculate that other unidentified glial paranodal junctional components may play a functional role redundant with that of ankyrins, or the clustering mechanism from the axonal paranodal cytoskeleton, including 4.1B, αII spectrin and βII

spectrin [1, 2, 19], may be sufficient to sustain paranodal junction assembly. However, paranodal junctions still form in 4.1B- and βII spectrin-KO mice[25-27, 50], consistent with the idea of robust and redundant mechanisms for paranodal junction formation. To test this possibility, it will be necessary to generate mice lacking both paranodal ankyrins and 4.1B or βII spectrin to determine if they show more severe defects than single KO mice.

Alternatively, the local environment at paranodal junctions may be sufficient to support the slow maturation of junctional NF155/Caspr/contactin complexes. Mature paranodal junctions have lipid raft-like properties [36], and paranodal proteins have features characteristic of proteins often found in lipid rafts[51]. For example, contactin is a glycosylphosphatidylinositol (GPI)-anchored protein and neurofascin forms a dimer and is palmitoylated[52, 53]. We previously proposed that when NF155 and Caspr/contactin complexes bind to each other at paranodes, lipid-raft lipid components are also recruited. The clustering of NF155/Caspr/contactin and lipid-raft lipid components mutually stabilize each other[36]. If this intrinsic mechanism is sufficient to constrain these CAMs within the special paranodal lipid environment, removal of glial cytoskeletal scaffolds may only cause a delay or mild defect in paranodal junction formation and no or mild defects in maintenance. Nevertheless, our results show that in the CNS, these ankyrin-independent mechanisms can only rescue late paranodal junction formation.

Although ankyrins are common to almost every cell in multicellular organisms and function as scaffolds, expression of ankyrins is remarkably complicated. First, ankyrins can be transcribed from several different alternative promoters, and different first exons encode their own stretches of peptide sequences. Second, ankyrin transcripts undergo extensive alternative splicing to produce various ankyrin protein isoforms[11]. AnkB and AnkG have alternative long exons whose incorporation makes giant versions of ankyrins. Giant AnkB and AnkG were thought to be exclusive to neurons[11, 12]. We consistently found myelinating glia utilize 220-kDa AnkB rather than its 440-kDa isoform. However, our analysis revealed that oligodendrocytes express both 190-kDa and 270-kDa AnkG. Why different ankyrin isoforms are expressed remains obscure since ankyrins generally function as scaffolds. However, one previous study showed that the protein domain specific to giant AnkG is required for its localization at the AIS[54], suggesting one purpose of the different isoforms may be to locate scaffolds in different membrane subdomains and perhaps also provide functional regulation for their assembly and maintenance. Future studies will be required to determine the functions of different ankyrin isoforms in these diverse cellular compartments.

AnkG has recently been implicated in psychiatric disorders including bipolar disorder, schizophrenia and autism by both association and sequencing studies[55-60]. In

addition to its crucial role at the AIS and nodes, our study reveals the importance of glial AnkG, and this pool of AnkG must be considered while the psychiatric etiology of the probable “AnkG syndromes” is pursued. In spite of the severe delay in paranodal junction assembly and reduced conduction velocity in the *AnkG-cKO* and *AnkB/G-cKO* mice, we observed no tremor or ataxia and many paranodal junctions had already formed by P21 (**Fig. 3j** and **4a**). However, a more detailed behavioral analysis may reveal how proper paranodal junction assembly affects activity-dependent circuit refinement during development, since the temporal pattern of neural activity should be altered by the reduced action potential conduction velocity in the *AnkG-cKO* and *AnkB/G-cKO* neonates.

In conclusion, our study genetically defined paranodal ankyrins as ankyrins contributed by myelinating glia. Our data support a model where paranodal ankyrins facilitate clustering and stabilization of paranodal CAM complexes to potentiate early formation of paranodal junctions in the CNS.

METHODS

Animals. The AnkB conventional KO mice were described previously[23] except that the genetic background was changed to C57BL/6. The Caspr KO[61], AnkG exon 1b KO[31], Neurofascin KO[37, 62] and *Cnp-Cre*[24] mice were described previously. Sprague-Dawley rats were purchased from Harlan Laboratories. *Ank2*^{floxed}: exon 24 (ENSMUSE00001285026 in Ensembl) is flanked by loxP sites (Peter, can you add details about the generation of the mice). *Ank3*^{floxed}: exons 23 and 24 (ENSMUSE00001261484 and ENSMUSE00001217354, respectively) are flanked by loxP sites[63].

Antibodies. The primary antibodies used were: rabbit antibodies against AnkB membrane-binding domain[18], AnkB C-terminal region (H-300, SantaCruz), AnkG spectrin-binding domain and C-terminal region[18], AnkG NT2 and NT3 were generated by immunizing against peptides unique to these domains followed by affinity purification of specific antibodies, AnkG 480/270[13], GFP (A11122, Life Technologies), NF-M (AB1987, Millipore), Caspr[36], βIV spectrin SD[64], Kv1.2[65], Caspr2 (ab33994, Abcam), Nav1.2[66], 4.1G[67]; mouse monoclonal antibodies against AnkB membrane-binding domain (N105/13 and N105/17, UC Davis/NIH NeuroMab Facility), AnkB spectrin-binding

domain (2.20, SantaCruz), AnkG spectrin-binding domain or C-terminal region (N106/36 and N106/65, NeuroMab), Caspr (K65/35, NeuroMab), actin (C4, Millipore), ZO-1 (ZO1-1A12, Life Technologies), E-cadherin (4A2C7, Life Technologies), Kv1.2 (K14/16, NeuroMab), Nav1.6 (K87A/10, NeuroMab), CNP (11-5B, Sigma-Aldrich), MAG (513, Millipore), Necl4 (N244/5, NeuroMab), pan-Nav channels (K58/35[20]) and GFP (N86/38, NeuroMab); the rat monoclonal antibody against MBP (MAB386, Millipore); chicken antibodies against NFasc (AF3235, R&D Systems) and βIV spectrin SD[68]; goat antibodies against contactin (AF904, R&D Systems) and AnkG (Vann, do you have a reference for this antibody?). The secondary antibodies were purchased from Life Technologies and Jackson ImmunoResearch.

DRG neuron-Schwann cell myelinating co-culture. Primary DRG neuron culture and Schwann cell culture were prepared from Sprague-Dawley rats as described previously[45]. The purified rat DRG neurons were infected with the adenovirus carrying the construct expressing AnkB shRNA and GFP[18] at 14 days *in vitro* (DIV). At 15 DIV, the whole culture medium was changed and the purified rat Schwann cells were added. Since 22 DIV, ascorbic acid had been included in the medium to induce myelination. The culture was fixed at 43 DIV (**Fig. 1b, c**) or 66 DIV (**Fig. 1d**) (21 or 44 days after induction

of myelination, respectively) and immunostained. The DRG neurons of the AnkB conventional KO were prepared from P0 neonates. The purified rat Schwann cells were added at 16 DIV; ascorbic acid had been included since 23 DIV. The co-culture was fixed and stained 28 days later (**Fig. 1f**).

Immunostaining was performed as described previously[5].

Electrophysiology. Compound action potentials were measured in a bath of Locke's solution with suction electrodes[20] or in vivo[69] as described.

Transmission electron microscopy was performed in Integrated Microscopy Core at Baylor College of Medicine as described prerviously[68].

Immunoprecipitation. Adult rat sciatic nerves were homogenized in Homogenizing buffer (320 mM sucrose, 5 mM sodium phosphate pH 7.2, 0.2 mM NaF, 0.2 mM Na_3VO_4, 2 × PhosSTOP (Roche), 2 μg/ml aprotinin, 1 μg/ml leupeptin, 2 μg/ml antipain, 10 μg/ml benzamidine and 0.5 mM PMSF) with sonication. The supernatant was collected after 700 × g centrifugation for 10 min at 4˚C. P21 mouse spinal cords were homogenized in

Homogenizing buffer with Dounce homogenizer. The supernatant from 700 × g centrifugation (10 min at 4˚C) was centrifuged again at 27200 × g for 90 min at 4˚C. The pellet was resuspended in Homogenizing buffer. The lysates used for immunoprecipitation were prepared by diluting sciatic nerve and spinal cord homogenates to final protein concentration at 1 mg/ml with Lysis buffer (1% (v/v) Triton X-100, 20 mM Tris-HCl pH 8.0, 10 mM EDTA, 150 mM NaCl, 10 mM NaN_3, 2 × PhosSTOP, 2 μg/ml aprotinin, 1 μg/ml leupeptin, 2 μg/ml antipain, 10 μg/ml benzamidine and 0.5 mM PMSF), supplementing Triton X-100 to totally 1%, mixing by a rotator for 1 hr at 4˚C, centrifuging at 13000 × g for 30 min at 4˚C and harvesting the supernatants. 16 μg of mouse monoclonal anti-AnkB N105/17 and anti-GFP N86/38 antibodies (for sciatic nerves) and 16 μg of mouse monoclonal anti-AnkG N106/36 and anti-GFP N86/38 antibodies (for spinal cords) were each incubated with 40 μl of protein A agarose (Thermo Scientific) in 300 μl of Lysis buffer for 1-2 hr. The beads were washed with 1 ml of Lysis buffer three times and then incubated with the lysates (650 μl for sciatic nerves and 620 μl for spinal cords) overnight at 4˚C. The beads were then washed with 1 ml of ice-cold Lysis buffer four times and subjected to Western blotting.

Quantitative reverse transcription-polymerase chain reaction (qRT-PCR). Total

RNA of P31 spinal cords and sciatic nerves were prepared by homogenizing tissues in TRIzol reagent (Life Technologies) and then purifying RNA with Direct-zol RNA MiniPrep (Zymo Research). 1 μg (from spinal cords) and 0.5 μg (from sciatic nerves) of total RNA were used in 20 μl of reverse transcription reaction with SuperScript III First-Strand Synthesis System (Life Technologies) in the presence or absence of the reverse transcriptase according to the manufacturer's instruction. The RT reaction was then diluted to 1/4 × and 2 μl were used for qPCR in 25 μl of reaction with Power SYBR Green PCR Master Mix and StepOnePlus Real-time PCR System (both from Life Technologies). The primers used in qPCR are as follows (sequences shown from 5′ to 3′): AnkB exon 25 (forward: ACCACTACCACGACTATCAC; reverse: GTAGTTCATGCCATCCAGG), AnkB 440-kDa (forward: GGAACCCAAATCCACAAGAG ; reverse: ACAGGAACTTCATTAACCAGG), AnkB 220-kDa (forward: CAACTTAAACATCACCCTGC ; reverse: AGTTCTCTTGCTAATTCTGTCC), AnkB exon 1″ (forward: ACCGAGGGAAGGAGTTC; reverse: GGAGAGCATTGAGTCCATTC), AnkB exon 1′ (forward: GCACATGGATTACAGTCTGAG; reverse: GCAGTTCTTCATGTCCCTG), AnkB exon 1 (forward: CTTCCCAAACTGTTCAAAATG; reverse: CCCCTTTCAGATATTCCACC), AnkB exon ′1 (forward: GGATGGAGCGGAAAAGAAA; reverse: CAGGTGGAGAGCATTGAG), AnkG exon 22

(forward: GTGAATGGGAACACAGCTC; reverse: TCATCGTTTCTGGGACATTC), AnkG exon 1a (forward: GCAGAGCCGAGTTCCTG; reverse: TGAATAACAGGATCCAAAGTCAC), AnkG exon 1e (forward: GTGAAGAGCCAAAGGAGAAG; reverse: TTGGAAGCAAGATGGAGTG), AnkG exon 1b (forward: AAAAGGAAACACCGCAAACG; reverse: CTCAGAGACCACTTCCACATG), AnkG 480-kDa (forward: AGTAGGAGGACTGGTCCG; reverse: AGTTGTGGCATTCTTTCCG), AnkG 270-kDa (forward: GCCATGTCTCCAGATGTTG; reverse: TCTGTCCAACTAAGTCCCAG), AnkG 190-kDa (forward: CTTTGCCTCCCTAGCTTTAC; reverse: the same as 270), and Polr2a (forward: CATCAAGAGAGTGCAGTTCG; reverse: CCATTAGTCCCCCAAGTTTG). Technical triplicates of each set of wild-type (WT), cHet and cKO tissues were performed and analyzed. Comparison of cHet with WT and cKO with cHet was carried out by one-sample two-tailed t tests and two-sample two-tailed t tests, respectively.

ACKNOWLEDGEMENTS **(Please let me know what grants you'd like referenced)**

This work was supported by grants from the NIH (NS069688 and NS044916) and

the Miriam and Sheldon G. Adelson Medical Research Foundation.

REFERENCES

1. Poliak, S. & Peles, E. The local differentiation of myelinated axons at nodes of Ranvier. *Nat Rev Neurosci* **4**, 968-980 (2003).

2. Salzer, J.L. Polarized domains of myelinated axons. *Neuron* **40**, 297-318 (2003).

3. Rosenbluth, J. Multiple functions of the paranodal junction of myelinated nerve fibers. *J Neurosci Res* **87**, 3250-3258 (2009).

4. Feinberg, K.*, et al.* A glial signal consisting of gliomedin and NrCAM clusters axonal Na^+ channels during the formation of nodes of Ranvier. *Neuron* **65**, 490-502 (2010).

5. Susuki, K.*, et al.* Three mechanisms assemble central nervous system nodes of Ranvier. *Neuron* **78**, 469-482 (2013).

6. Rios, J.C.*, et al.* Paranodal interactions regulate expression of sodium channel subtypes and provide a diffusion barrier for the node of Ranvier. *J Neurosci* **23**, 7001-7011 (2003).

7. Babbs, C.F. & Shi, R. Subtle paranodal injury slows impulse conduction in a mathematical model of myelinated axons. *PLoS One* **8**, e67767 (2013).

8. Bhat, M.A.*, et al.* Axon-glia interactions and the domain organization of myelinated

axons requires neurexin IV/Caspr/Paranodin. *Neuron* **30**, 369-383 (2001).

9. Boyle, M.E.*, et al.* Contactin orchestrates assembly of the septate-like junctions at the paranode in myelinated peripheral nerve. *Neuron* **30**, 385-397 (2001).

10. Pillai, A.M.*, et al.* Spatiotemporal ablation of myelinating glia-specific *Neurofascin* (*Nfasc*^{NF155}) in mice reveals gradual loss of paranodal axoglial junctions and concomitant disorganization of axonal domains. *J Neurosci Res* **87**, 1773-1793 (2009).

11. Bennett, V. & Baines, A.J. Spectrin and ankyrin-based pathways: metazoan inventions for integrating cells into tissues. *Physiol Rev* **81**, 1353-1392 (2001).

12. Bennett, V. & Healy, J. Membrane domains based on ankyrin and spectrin associated with cell-cell interactions. *Cold Spring Harbor perspectives in biology* **1**, a003012 (2009).

13. Kordeli, E., Lambert, S. & Bennett, V. Ankyrin$_G$. A new ankyrin gene with neural-specific isoforms localized at the axonal initial segment and node of Ranvier. *J Biol Chem* **270**, 2352-2359 (1995).

14. Dzhashiashvili, Y.*, et al.* Nodes of Ranvier and axon initial segments are ankyrin G-dependent domains that assemble by distinct mechanisms. *J Cell Biol* **177**, 857-870 (2007).

15. Rasband, M.N. The axon initial segment and the maintenance of neuronal polarity.

Nat Rev Neurosci **11**, 552-562 (2010).

16. Gasser, A.*, et al.* An ankyrinG-binding motif is necessary and sufficient for targeting $Na_v1.6$ sodium channels to axon initial segments and nodes of Ranvier. *J Neurosci* **32**, 7232-7243 (2012).

17. Chan, W., Kordeli, E. & Bennett, V. 440-kD $ankyrin_B$: structure of the major developmentally regulated domain and selective localization in unmyelinated axons. *J Cell Biol* **123**, 1463-1473 (1993).

18. Galiano, M.R.*, et al.* A distal axonal cytoskeleton forms an intra-axonal boundary that controls axon initial segment assembly. *Cell* **149**, 1125-1139 (2012).

19. Ogawa, Y.*, et al.* Spectrins and ankyrinB constitute a specialized paranodal cytoskeleton. *J Neurosci* **26**, 5230-5239 (2006).

20. Rasband, M.N.*, et al.* Dependence of nodal sodium channel clustering on paranodal axoglial contact in the developing CNS. *J Neurosci* **19**, 7516-7528 (1999).

21. Jenkins, S.M. & Bennett, V. Developing nodes of Ranvier are defined by ankyrin-G clustering and are independent of paranodal axoglial adhesion. *Proc Natl Acad Sci U S A* **99**, 2303-2308 (2002).

22. Cahoy, J.D.*, et al.* A transcriptome database for astrocytes, neurons, and oligodendrocytes: a new resource for understanding brain development and function. *J*

Neurosci **28**, 264-278 (2008).

23. Scotland, P., Zhou, D., Benveniste, H. & Bennett, V. Nervous system defects of $Ankyrin_B$ (-/-) mice suggest functional overlap between the cell adhesion molecule L1 and 440-kD $Ankyrin_B$ in premyelinated axons. *J Cell Biol* **143**, 1305-1315 (1998).

24. Lappe-Siefke, C.*, et al.* Disruption of *Cnp1* uncouples oligodendroglial functions in axonal support and myelination. *Nature genetics* **33**, 366-374 (2003).

25. Horresh, I., Bar, V., Kissil, J.L. & Peles, E. Organization of myelinated axons by Caspr and Caspr2 requires the cytoskeletal adapter protein 4.1B. *J Neurosci* **30**, 2480-2489 (2010).

26. Cifuentes-Diaz, C.*, et al.* Protein 4.1B contributes to the organization of peripheral myelinated axons. *PLoS One* **6**, e25043 (2011).

27. Zhang, C., Susuki, K., Zollinger, D.R., Dupree, J.L. & Rasband, M.N. Membrane domain organization of myelinated axons requires βII spectrin. *J Cell Biol* **203**, 437-443 (2013).

28. Hoshi, T.*, et al.* Nodal protrusions, increased Schmidt-Lanterman incisures, and paranodal disorganization are characteristic features of sulfatide-deficient peripheral nerves. *Glia* **55**, 584-594 (2007).

29. Hedstrom, K.L.*, et al.* Neurofascin assembles a specialized extracellular matrix at

the axon initial segment. *J Cell Biol* **178**, 875-886 (2007).

30. Hedstrom, K.L., Ogawa, Y. & Rasband, M.N. AnkyrinG is required for maintenance of the axon initial segment and neuronal polarity. *J Cell Biol* **183**, 635-640 (2008).

31. Zhou, D.*, et al.* $Ankyrin_G$ is required for clustering of voltage-gated Na channels at axon initial segments and for normal action potential firing. *J Cell Biol* **143**, 1295-1304 (1998).

32. Sobotzik, J.M.*, et al.* AnkyrinG is required to maintain axo-dendritic polarity in vivo. *Proc Natl Acad Sci U S A* **106**, 17564-17569 (2009).

33. Garver, T.D., Ren, Q., Tuvia, S. & Bennett, V. Tyrosine phosphorylation at a site highly conserved in the L1 family of cell adhesion molecules abolishes ankyrin binding and increases lateral mobility of neurofascin. *J Cell Biol* **137**, 703-714 (1997).

34. Tuvia, S., Garver, T.D. & Bennett, V. The phosphorylation state of the FIGQY tyrosine of neurofascin determines ankyrin-binding activity and patterns of cell segregation. *Proc Natl Acad Sci U S A* **94**, 12957-12962 (1997).

35. Jenkins, S.M.*, et al.* FIGQY phosphorylation defines discrete populations of L1 cell adhesion molecules at sites of cell-cell contact and in migrating neurons. *Journal of cell science* **114**, 3823-3835 (2001).

36. Schafer, D.P., Bansal, R., Hedstrom, K.L., Pfeiffer, S.E. & Rasband, M.N. Does

paranode formation and maintenance require partitioning of neurofascin 155 into lipid rafts? *J Neurosci* **24**, 3176-3185 (2004).

37. Zonta, B.*, et al.* Glial and neuronal isoforms of Neurofascin have distinct roles in the assembly of nodes of Ranvier in the central nervous system. *J Cell Biol* **181**, 1169-1177 (2008).

38. Kunimoto, M. A neuron-specific isoform of brain ankyrin, 440-kD ankyrin$_B$, is targeted to the axons of rat cerebellar neurons. *J Cell Biol* **131**, 1821-1829 (1995).

39. Cunha, S.R., Le Scouarnec, S., Schott, J.J. & Mohler, P.J. Exon organization and novel alternative splicing of the human *ANK2* gene: implications for cardiac function and human cardiac disease. *Journal of molecular and cellular cardiology* **45**, 724-734 (2008).

40. Rueckert, E.H.*, et al. Cis*-acting regulation of brain-specific *ANK3* gene expression by a genetic variant associated with bipolar disorder. *Molecular psychiatry* **18**, 922-929 (2013).

41. Hopitzan, A.A., Baines, A.J., Ludosky, M.A., Recouvreur, M. & Kordeli, E. Ankyrin-G in skeletal muscle: Tissue-specific alternative splicing contributes to the complexity of the sarcolemmal cytoskeleton. *Experimental cell research* **309**, 86-98 (2005).

42. Davis, J.Q., Lambert, S. & Bennett, V. Molecular composition of the node of Ranvier: identification of ankyrin-binding cell adhesion molecules neurofascin

(mucin+/third FNIII domain-) and NrCAM at nodal axon segments. *J Cell Biol* **135**, 1355-1367 (1996).

43. Tait, S.*, et al.* An oligodendrocyte cell adhesion molecule at the site of assembly of the paranodal axo-glial junction. *J Cell Biol* **150**, 657-666 (2000).

44. Susuki, K. & Rasband, M.N. Spectrin and ankyrin-based cytoskeletons at polarized domains in myelinated axons. *Experimental biology and medicine* **233**, 394-400 (2008).

45. Susuki, K.*, et al.* Schwann cell spectrins modulate peripheral nerve myelination. *Proc Natl Acad Sci U S A* **108**, 8009-8014 (2011).

46. Hammarlund, M., Jorgensen, E.M. & Bastiani, M.J. Axons break in animals lacking β-spectrin. *J Cell Biol* **176**, 269-275 (2007).

47. Xu, K., Zhong, G. & Zhuang, X. Actin, spectrin, and associated proteins form a periodic cytoskeletal structure in axons. *Science* **339**, 452-456 (2013).

48. Chang, K.J. & Rasband, M.N. Excitable domains of myelinated nerves: axon initial segments and nodes of Ranvier. *Curr Top Membr* **72**, 159-192 (2013).

49. Eisenbach, M.*, et al.* Differential clustering of Caspr by oligodendrocytes and Schwann cells. *J Neurosci Res* **87**, 3492-3501 (2009).

50. Einheber, S.*, et al.* The 4.1B cytoskeletal protein regulates the domain organization and sheath thickness of myelinated axons. *Glia* **61**, 240-253 (2013).

51. Munro, S. Lipid rafts: elusive or illusive? *Cell* **115**, 377-388 (2003).

52. Zhang, X., Davis, J.Q., Carpenter, S. & Bennett, V. Structural requirements for association of neurofascin with ankyrin. *J Biol Chem* **273**, 30785-30794 (1998).

53. Ren, Q. & Bennett, V. Palmitoylation of neurofascin at a site in the membrane-spanning domain highly conserved among the L1 family of cell adhesion molecules. *Journal of neurochemistry* **70**, 1839-1849 (1998).

54. Zhang, X. & Bennett, V. Restriction of 480/270-kD ankyrin G to axon proximal segments requires multiple ankyrin G-specific domains. *J Cell Biol* **142**, 1571-1581 (1998).

55. Shi, L.*, et al.* Whole-genome sequencing in an autism multiplex family. *Molecular autism* **4**, 8 (2013).

56. Ferreira, M.A.*, et al.* Collaborative genome-wide association analysis supports a role for *ANK3* and *CACNA1C* in bipolar disorder. *Nature genetics* **40**, 1056-1058 (2008).

57. Schulze, T.G.*, et al.* Two variants in *Ankyrin 3 (ANK3)* are independent genetic risk factors for bipolar disorder. *Molecular psychiatry* **14**, 487-491 (2009).

58. Iqbal, Z.*, et al.* Homozygous and heterozygous disruptions of *ANK3*: at the crossroads of neurodevelopmental and psychiatric disorders. *Human molecular genetics* **22**, 1960-1970 (2013).

59. Yuan, A.*, et al. ANK3* as a risk gene for schizophrenia: new data in Han Chinese and meta analysis. *American journal of medical genetics. Part B, Neuropsychiatric genetics : the official publication of the International Society of Psychiatric Genetics* **159B**, 997-1005 (2012).

60. Gella, A.*, et al.* Is Ankyrin a genetic risk factor for psychiatric phenotypes? *BMC psychiatry* **11**, 103 (2011).

61. Gollan, L., Salomon, D., Salzer, J.L. & Peles, E. Caspr regulates the processing of contactin and inhibits its binding to neurofascin. *J Cell Biol* **163**, 1213-1218 (2003).

62. Sherman, D.L.*, et al.* Neurofascins are required to establish axonal domains for saltatory conduction. *Neuron* **48**, 737-742 (2005).

63. Jenkins, P.M.*, et al.* E-cadherin polarity is determined by a multifunction motif mediating lateral membrane retention through ankyrin-G and apical-lateral transcytosis through clathrin. *J Biol Chem* **288**, 14018-14031 (2013).

64. Yang, Y., Lacas-Gervais, S., Morest, D.K., Solimena, M. & Rasband, M.N. βIV spectrins are essential for membrane stability and the molecular organization of nodes of Ranvier. *J Neurosci* **24**, 7230-7240 (2004).

65. Rhodes, K.J., Keilbaugh, S.A., Barrezueta, N.X., Lopez, K.L. & Trimmer, J.S. Association and colocalization of K^+ channel α- and β-subunit polypeptides in rat brain. *J*

Neurosci **15**, 5360-5371 (1995).

66. Schafer, D.P., Custer, A.W., Shrager, P. & Rasband, M.N. Early events in node of Ranvier formation during myelination and remyelination in the PNS. *Neuron Glia Biol* **2**, 69-79 (2006).

67. Ivanovic, A.*, et al.* The cytoskeletal adapter protein 4.1G organizes the internodes in peripheral myelinated nerves. *J Cell Biol* **196**, 337-344 (2012).

68. Chang, K.J., Susuki, K., Dours-Zimmermann, M.T., Zimmermann, D.R. & Rasband, M.N. Oligodendrocyte myelin glycoprotein does not influence node of Ranvier structure or assembly. *J Neurosci* **30**, 14476-14481 (2010).

69. Susuki, K.*, et al.* Gangliosides contribute to stability of paranodal junctions and ion channel clusters in myelinated nerve fibers. *Glia* **55**, 746-757 (2007).

FIGURE LEGENDS

Figure 1. Paranodal AnkB is derived from Schwann cells in the peripheral nervous system. (**a**) Immunostaining of a mouse sciatic nerve with antibodies against AnkG (green, node) and AnkB (red, paranodes). (**b**) Cultured DRG neurons were infected with adenovirus carrying a GFP and AnkB shRNA-expressing construct, and immunostained with antibodies against GFP (green) and AnkB (red). The GFP-positive axon is indicated by arrowheads. (**c,d**) Schwann cells were added to the same culture as in (**b**) and induced to myelinate. The co-culture was labeled for myelin basic protein (MBP, blue), GFP (green) and AnkB (red). The arrow points to paranodal AnkB (**c**). (**e**) Immunoblot of lysates from rat hippocampal neuron and purified Schwann cell cultures probed with anti-AnkB and anti-actin antibodies. (**f**) DRG neurons from the AnkB conventional KO were co-cultured with myelinating rat Schwann cells and labeled for AnkB (red), MBP (green) and neurofilament-M (NF-M, blue). The arrow points to paranodal accumulation of AnkB. Localization of AnkB along the inner mesaxon[19] was also observed as spiral extensions from paranodal junctions. (**g**) The scheme of the *Ank2* conditional allele. The two loxP sites (red triangles) flank exon 24. After Cre recombination and removal of exon 24, a premature stop codon is generated in exon 25. (**h,i**) Immunostaining of sciatic nerve longitudinal sections from 4-week-old *AnkB-cHet* (**h**) and *AnkB-cKO* (**i**) with

antibodies against AnkB (red) and Caspr (green). Arrows point to paranodal junctions. Scale bars = 5 μm (**a**), and 10 μm (**b-d,f**), and 5 μm (**h,i**).

Figure 2. No paranodal or axonal abnormalities were observed in sciatic nerves of *AnkB-cKO* mice. (**a-i, k-m**) Immunostaining of sciatic nerve longitudinal sections from 4 to 6-week-old (**a-l, m**), P3 (**k**) and 1-year-old (**l**) mice shows normal paranodal and juxtaparanodal domains and proper Nav channel subtype switch in *AnkB-cKO* mice. NFasc, neurofascin (both nodal 186-kDa and paranodal 155-kDa isoforms were stained). Cntn, contactin. βIV, βIV spectrin. ZO-1, zona occludens protein 1. MAG, myelin-associated glycoprotein. CNP, 2',3'-cyclic nucleotide 3' phosphodiesterase. Necl4, nectin-like protein 4. (**j**) Conduction velocities of 6 P56 sciatic nerves from each genotype were measured using suction electrodes. ns, not significant. Scale bars = 5 μm (**a,b**), 5 μm (**c-g**), 5 μm (**h**), 5 μm (**i**), 5 μm (**k**), 5 μm (**l**), and 5 μm (**m**).

Figure 3. Paranodal junction assembly is disrupted in *AnkG-cKO* mice. (**a**) The dorsal root entry zone from a P31 mouse spinal cord immunostained with antibodies against AnkB (green), AnkG (red) and βIV spectrin (βIV, cyan). PNS and CNS label the parts of the axon before and after its entry into the spinal cord, respectively. (**b**) The scheme of

the *Ank3* conditional allele. The two loxP sites (red triangles) flank exons 23 and 24. After Cre recombination and removal of exons 23 and 24, a premature stop codon is generated in exon 25. (**c-e**) Immunostaining of P22 optic nerves with antibodies against AnkG (red) and βIV spectrin (green). Arrowheads point to paranodes. (**f, g**) Immunostaining of P12 optic nerves labeled for Caspr (green) and βIV spectrin (red). Arrows point to three nodal clusters of βIV spectrin without accompanying paranodal junctions. (**h**) Quantification of the percentages of full nodes and nodal intermediates (paranodes only, nodes alone and heminodes) in P12 optic nerves. (**i,j**) Conduction of compound action potentials along P17 optic nerves was measured using suction electrodes. The average peak velocities for each genotype is shown in (**j**). ns, not significant. **, $p < 0.01$. ***, $p < 0.001$. Scale bars = 5 μm (**a**), 3 μm (**c-e**), and 5 μm (**f,g**).

Figure 4. Paranodal junctions recover over time in the CNS of the *AnkG-cKO* and *AnkB/G-cKO* mice. (**a**) Quantification of the percentages of full nodes and nodal intermediates (paranodes only, nodes alone and heminodes) in P12, P17, P21 and P56 optic nerves. WT, wild type. G cKO, *AnkG-cKO*. B cKO, *AnkB-cKO*. B/G cKO, *AnkB/G-cKO*. The data for P12 WT and G cKO are the same as those shown in **Fig. 3h**. (**b,c**) Immunostaining of optic nerves from P22 (**a**) and 1-year-old (**b**) mice. (**d,e**)

Immunostaining of P22 optic nerves with anti-AnkB (red) and anti-Caspr (green) antibodies. (**f,g**) Immunostaining of P12 optic nerves with antibodies against Caspr (green) and βIV spectrin (red). (**h,i**) Immunostaining of P21 optic nerves with antibodies against NFasc (green), Kv1.2 channel (red) and βIV spectrin (blue). (**j**) Electron micrographs of P17 optic nerve cross sections. (**k**) Quantification of the percentage of axons in each diameter range that were myelinated. (**l**) Quantification of the percentage of total axons that belonged to different groups of diameter ranges. Scale bars = 3 μm (**b**), 3 μm (**c**), 5 μm (**d,e**), 5 μm (**f,g**), 5 μm (**h,i**), and 1 μm (**j**).

Figure 5. AnkB and AnkG interact with NF155 *in vivo* and are targeted to paranodes independently of paranodal junctions and NF155. (**a-d**) P7 sciatic nerve sections stained for AnkB (red), NFasc (green) and Caspr (blue) (**a,c**), and the respective longitudinal line scans are shown (**b,d**). (**e**) Immunoprecipitation of AnkB from adult rat sciatic nerves co-precipitated NF155. Immunoprecipitation with the anti-GFP antibody served as a negative control. Heavy chain, mouse IgG heavy chain. (**f**) Immunoprecipitation of AnkG from P21 mouse spinal cords co-precipitated NF186 and NF155. (**g-i**) Immunostaining of P7 sciatic nerves with antibodies against AnkB (red) and NFasc (green). Arrows point to the residual AnkB and NFasc at paranodes. (**j,k**) Immunostaining of P7 spinal cords with

antibodies against AnkG (green) and NFasc (red). Arrows point to the residual AnkG and NFasc at paranodes. (**l-n**) Immunostaining of P5 sciatic nerves with antibodies against AnkB (red) and MAG (green). Arrows point to the paranodes with residual AnkB. Scale bars = (**a,c**) 5 μm for (a) and 3.3 μm for (c); 5 μm (**g-i**); 5 μm (**j,k**); 5 μm (**l-n**).

Figure 6. Schwann cells and oligodendrocytes express 220-kDa isoform of AnkB from multiple promoters. (**a**) qRT-PCR analysis of P31 sciatic nerves shows the transcript levels relative to *Ank2*$^{f/f}$ after normalization to Polr2a as the internal control. N= 4 for all genotypes analyzed. (**b**) Immunoblots of adult sciatic nerves homogenates probed with anti-AnkB and anti-actin antibodies. (**c**) qRT-PCR analysis of P31 spinal cords shows the transcript levels relative to *Ank2*$^{f/f}$ after normalization to Polr2a as the internal control. N= 4 for all genotypes analyzed. (**d**) Western blotting of membrane homogenates from P42 spinal cords probed with anti-AnkB and anti-actin antibodies. (**e**) The schema shows the alternative first exons from different promoters and alternative splicing of exon 40 of *Ank2*.

Figure 7. Oligodendrocytes express the 270-kDa and 190-kDa isoforms of AnkG from the promoter upstream to exon 1b. (**a**) qRT-PCR analysis of P31 spinal cords shows the

transcript levels relative to *Ank3*$^{f/f}$ after normalization to Polr2a as the internal control. N= 3 for all genotypes analyzed. (**b**) Immunoblotting of membrane homogenates from P31 spinal cords probed with anti-AnkG and anti-neurofilament M (NF-M) antibodies. (**c**) Immunostaining of P22 spinal cords with antibodies against 480/270-kDa AnkG isoforms (green) and Caspr (red). (**d**) Immunostaining of P22 spinal cords with antibodies against the peptide sequence encoded by *Ank3* exon 1e or 1b (green) and βIV spectrin (red). (**e**) P90 brain stems were labeled for AnkG (by N106/36, green) and Caspr (red). (**f**) The schema shows the alternative first exons from different promoters and alternative splicing of exon 41 of *Ank3*. Scale bars = 5 μm (**c**), 3 μm (**d**), and 2.5 μm (**e**).

Supplementary Figure 1. (**a**) The molecular architecture of nodes of Ranvier and paranodes including membrane proteins and cytoskeletal scaffolds. Paranodal ankyrins are located in myelinating glia and interact with NF155. Schwann cells in the PNS express AnkB (B) whereas oligodendrocytes in the CNS mainly express AnkG (G). The shorter tail of paranodal AnkG symbolizes 190-kDa and 270-kDa isoforms and the longer tail of nodal AnkG designates 480-kDa and 270-kDa isoforms. Cntn, contactin. αII/βII, αII/βII spectrin tetramer. βIV, βIV spectrin. (**b**) The cartoon illustrates the differential timing of formation of nodes (red) and paranodal junctions (green) in the PNS, CNS and

AnkB/G-cKO CNS.

Supplementary Table 1. The exon nomenclature of *Ank2* used in this study. The exon information was collected from a previous study[39] and the current information in the Ensembl database. The coordinates of each exon in chromosome 3 are shown. Except for the alternative first exons, all other known alternative exons are highlighted in yellow. Exons 2′ and 3′ are incorporated when exon 1′ is used. In this situation, exon 3′ is an alternative exon. When exon 1s is used, the predicted start codon is highlighted in red in exon 25. When exon 51 is included, the alternative stop codon is highlighted in red in exon 52.

Supplementary Table 2. The exon nomenclature of *Ank3* used in this study. The exon information was collected from a previous study[40] and the current information in the Ensembl database. The coordinates of each exon in chromosome 10 are shown. Except for the alternative first exons, all other known alternative exons are highlighted in yellow. Exon 2a is incorporated when exon 1a is used.

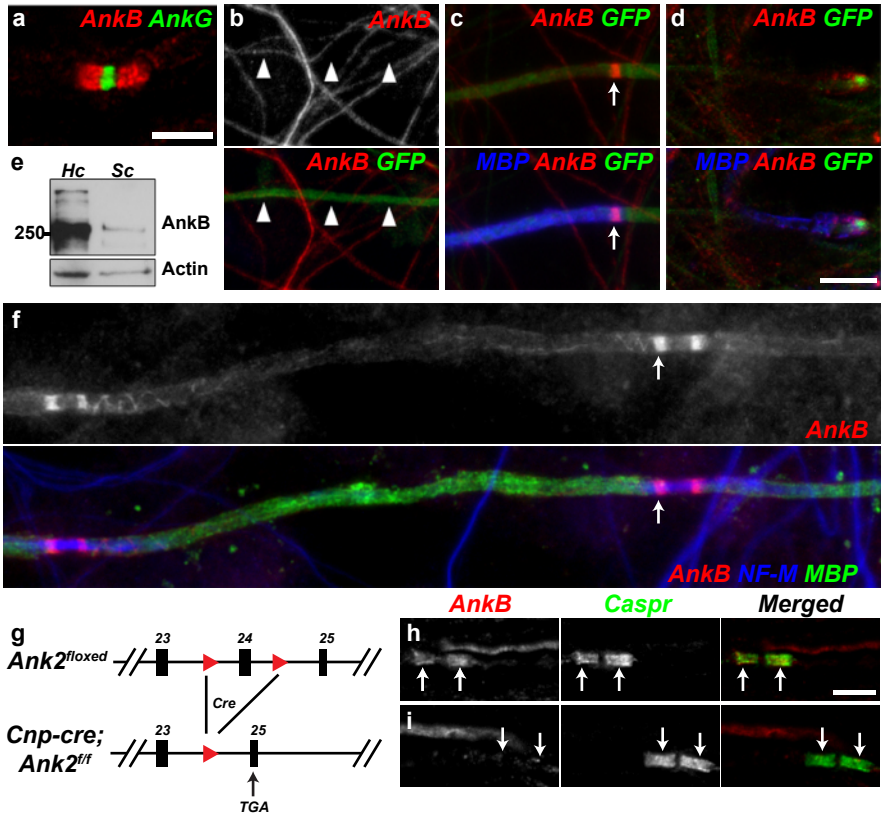
a
AnkB AnkG
b
AnkB
c
AnkB GFP
d
AnkB GFP
e
Hc
Sc
250
AnkB
Actin
AnkB GFP
MBP AnkB GFP
MBP AnkB GFP
f
AnkB
AnkB NF-M MBP
g
Ank2floxed
23
24
25
Cre
Cnp-cre;
Ank2f/f
23
25
TGA
AnkB
Caspr
Merged
h
i

Figure 1.

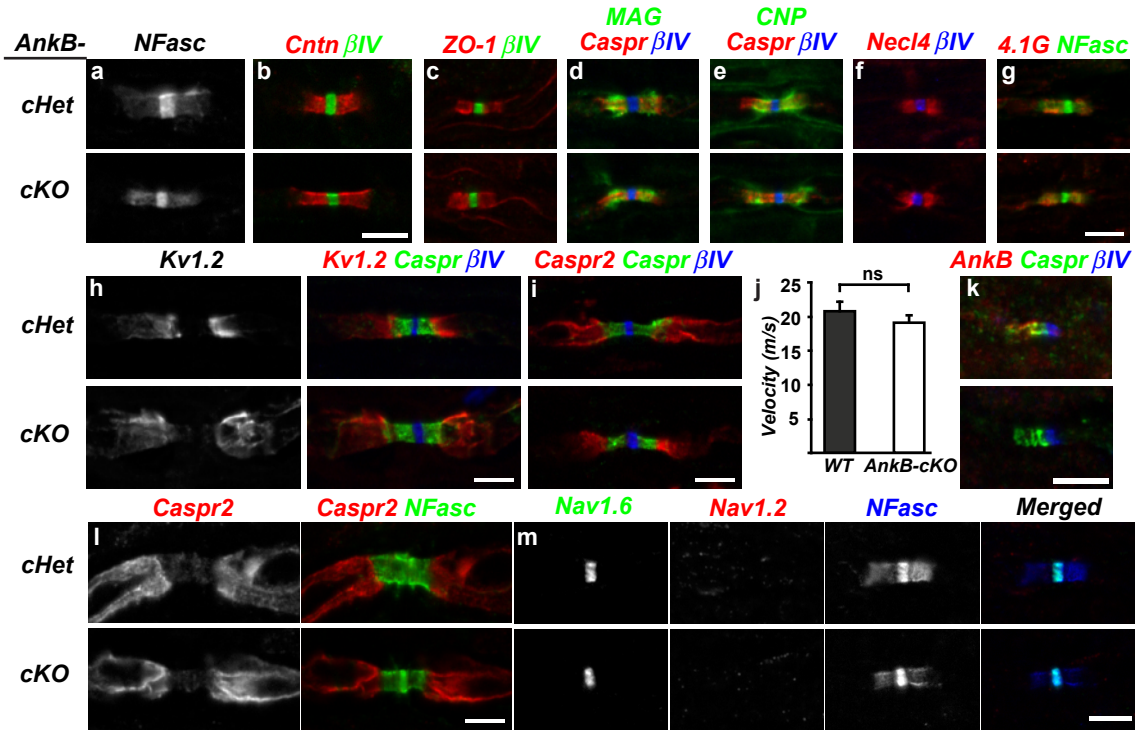
AnkB-
NFasc
Cntn βIV
ZO-1 βIV
MAG
Caspr βIV
CNP
Caspr βIV
Necl4 βIV
4.1G NFasc
a
b
c
d
e
f
g
cHet
cKO
Kv1.2
Kv1.2 Caspr βIV
Caspr2 Caspr βIV
AnkB Caspr βIV
h
i
j
k
ns
25
20
15
10
5
Velocity (m/s)
WT
AnkB-cKO
Caspr2
Caspr2 NFasc
Nav1.6
Nav1.2
NFasc
Merged
l
m

Figure 2.

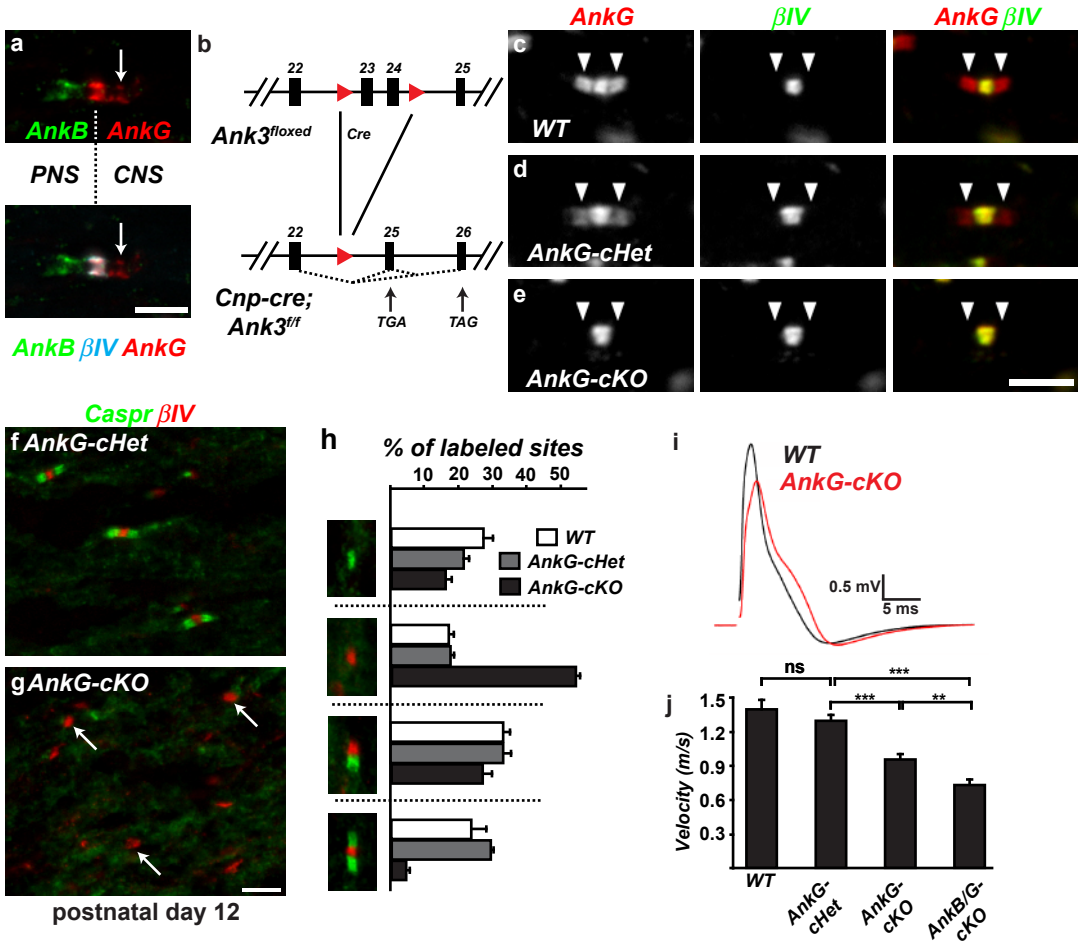
a
AnkB
AnkG
PNS
CNS
AnkB βIV AnkG
b
Ank3floxed
Cre
22
23
24
25
22
25
26
Cnp-cre;
Ank3f/f
TGA
TAG
AnkG
βIV
AnkG βIV
c
WT
d
AnkG-cHet
e
AnkG-cKO
Caspr βIV
f AnkG-cHet
g AnkG-cKO
postnatal day 12
h
% of labeled sites
10 20 30 40 50
WT
AnkG-cHet
AnkG-cKO
i
WT
AnkG-cKO
0.5 mV
5 ms
j
ns
***
***
**
Velocity (m/s)
1.5
1.2
0.9
0.6
0.3
WT
AnkG-cHet
AnkG-cKO
AnkB/G-cKO

Figure 3.

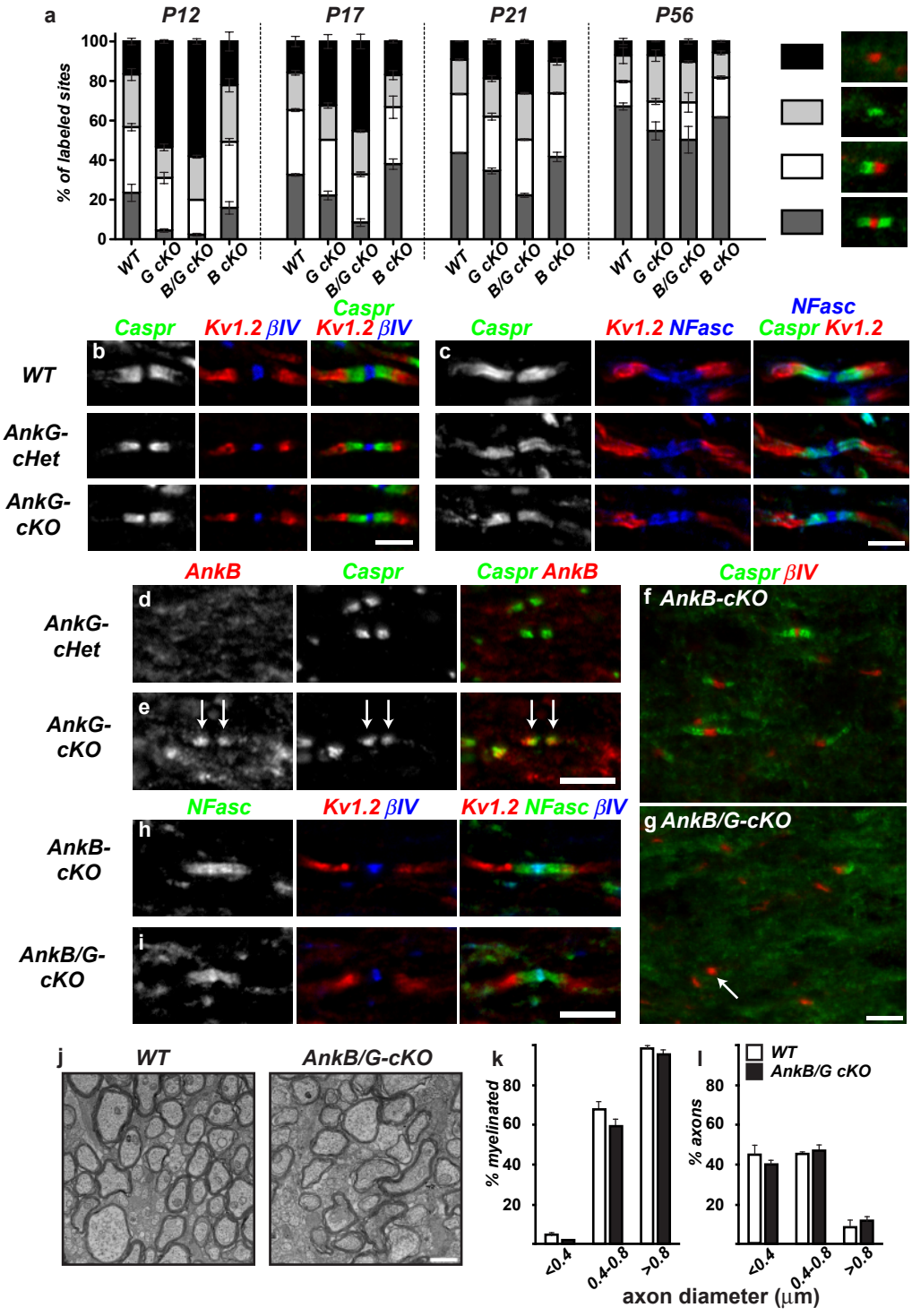
a
P12
P17
P21
P56
% of labeled sites
100
80
60
40
20
0
WT
G cKO
B/G cKO
B cKO
Caspr
Kv1.2 βIV
Caspr
Kv1.2 βIV
Caspr
Kv1.2 NFasc
NFasc
Caspr Kv1.2
b
c
WT
AnkG-cHet
AnkG-cKO
AnkB
Caspr
Caspr AnkB
Caspr βIV
d
f AnkB-cKO
AnkG-cHet
e
AnkG-cKO
NFasc
Kv1.2 βIV
Kv1.2 NFasc βIV
h
g AnkB/G-cKO
AnkB-cKO
i
AnkB/G-cKO
j
WT
AnkB/G-cKO
k
% myelinated
l
WT
AnkB/G cKO
% axons
<0.4
0.4-0.8
>0.8
axon diameter (μm)

Figure 4.

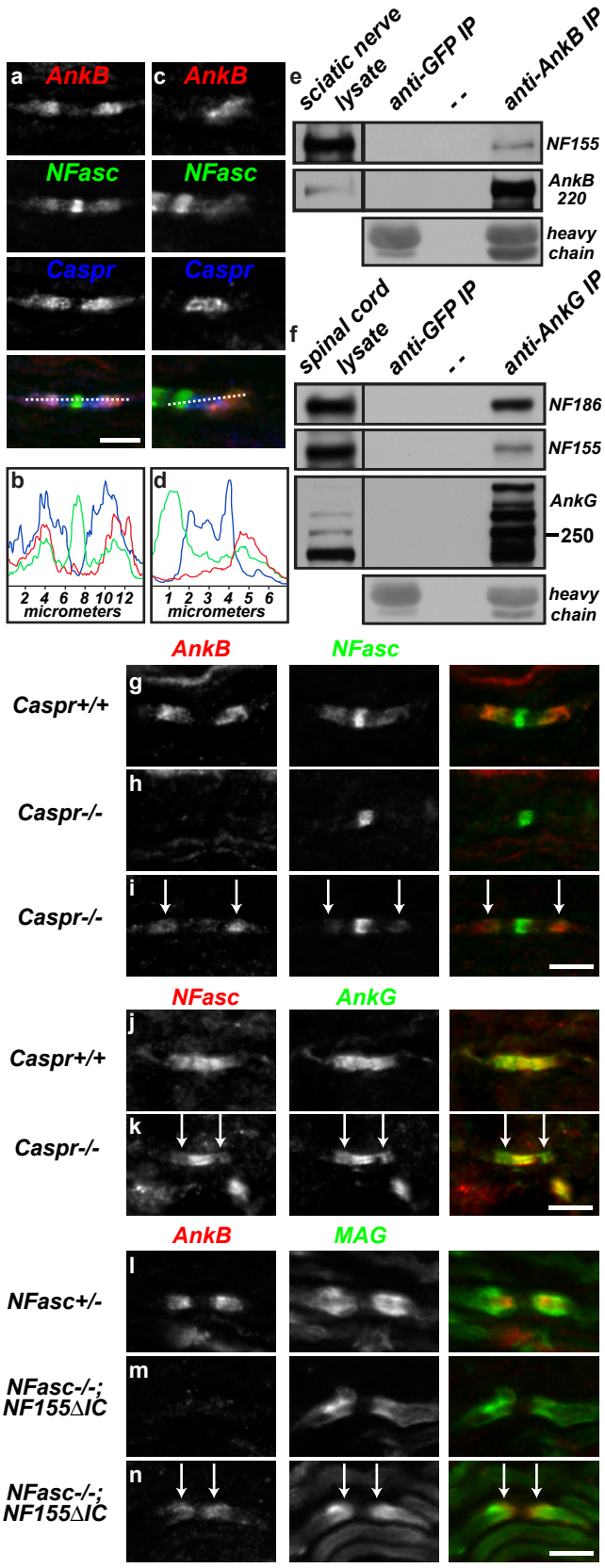
a AnkB
NFasc
Caspr
c AnkB
NFasc
Caspr
b
2 4 6 8 10 12
micrometers
d
1 2 3 4 5 6
micrometers
e
sciatic nerve lysate
anti-GFP IP
--
anti-AnkB IP
NF155
AnkB 220
heavy chain
f
spinal cord lysate
anti-GFP IP
--
anti-AnkG IP
NF186
NF155
AnkG
250
heavy chain
AnkB
NFasc
Caspr+/+
g
Caspr-/-
h
Caspr-/-
i
NFasc
AnkG
Caspr+/+
j
Caspr-/-
k
AnkB
MAG
NFasc+/-
l
NFasc-/-; NF155ΔIC
m
NFasc-/-; NF155ΔIC
n

Figure 5.

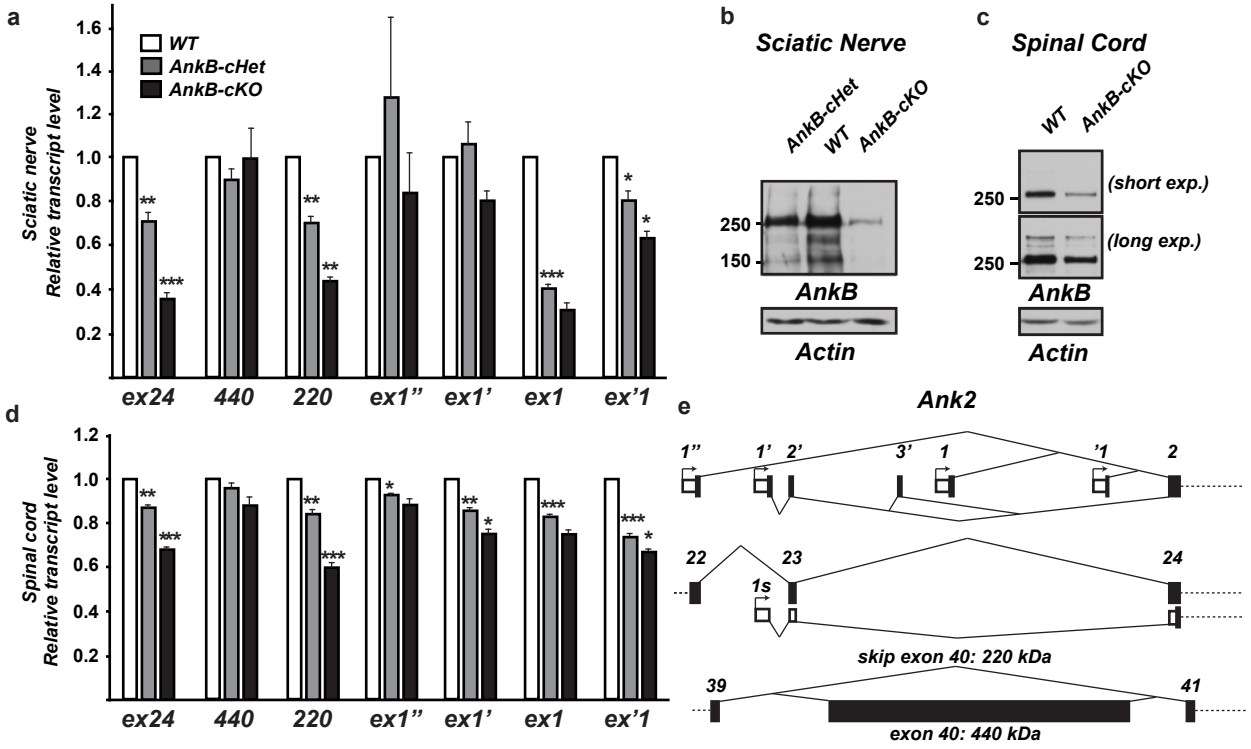
a
WT
AnkB-cHet
AnkB-cKO
Sciatic nerve
Relative transcript level
1.6
1.4
1.2
1.0
0.8
0.6
0.4
0.2
ex24
440
220
ex1''
ex1'
ex1
ex'1
b
Sciatic Nerve
AnkB-cHet
WT
AnkB-cKO
250
150
AnkB
Actin
c
Spinal Cord
WT
AnkB-cKO
(short exp.)
(long exp.)
250
250
AnkB
Actin
d
Spinal cord
Relative transcript level
1.2
1.0
0.8
0.6
0.4
0.2
ex24
440
220
ex1''
ex1'
ex1
ex'1
e
Ank2
1''
1'
2'
3'
1
'1
2
22
23
1s
24
skip exon 40: 220 kDa
39
41
exon 40: 440 kDa

Figure 6.

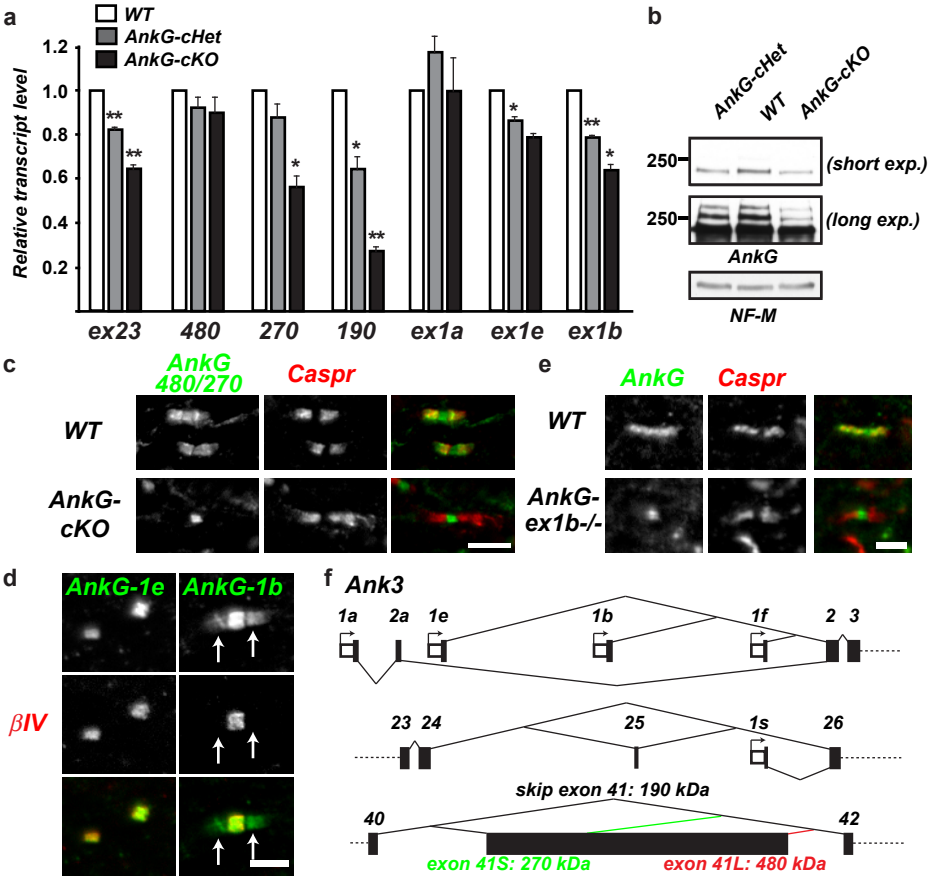
a
WT
AnkG-cHet
AnkG-cKO
Relative transcript level
1.2
1.0
0.8
0.6
0.4
0.2
ex23
480
270
190
ex1a
ex1e
ex1b
b
AnkG-cHet
WT
AnkG-cKO
250
(short exp.)
250
(long exp.)
AnkG
NF-M
c
AnkG 480/270
Caspr
WT
AnkG-cKO
e
AnkG
Caspr
WT
AnkG-ex1b-/-
d
AnkG-1e
AnkG-1b
βIV
f
Ank3
1a
2a
1e
1b
1f
2
3
23
24
25
1s
26
skip exon 41: 190 kDa
40
42
exon 41S: 270 kDa
exon 41L: 480 kDa

Figure 7.

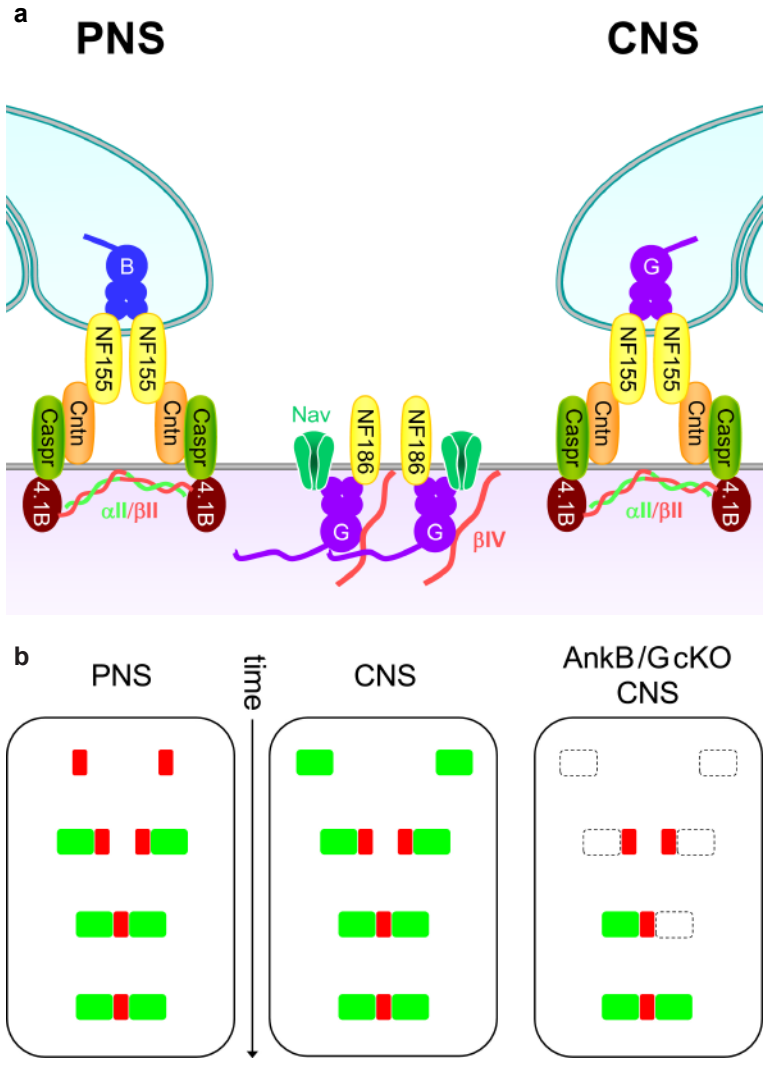

Supplementary Figure 1.

Exon No.		Start	End	Start Phase	End Phase	Length	Sequence
1´´	ENSMUSE00001205851	127,499,115	127,498,668	-	0	448	GAGCTCCGGCAGGCAGTGGTGCATATAGACATATTTCTGGGAGCTGTCCATGAGCTCATCGCTCTCCCGGCGCGCGGCGAAGGAAGAAGCCCTCCTCTTTCT CCCCGCGCCACCAGCAGCAGTCGCTTAGCGCTTGTCGCCGGCCCAGCCCGCAGCCCACTCGGCGCACCATGGCCCCACGGCACCTCGCGCAGAGGTAGGTGG GCTCGGGCAGCAGGTCTCCACGGGCGATCGCGGCCAAGGCCGACCTTCTGCGGTCGCCTAGAAGCACGCGGGTCCCCGGGTGAGCCCGAACGCCGCAGGCCG GGAGCGGAAGAGACGAGGACACGCGGGACAGCCGGACTTGACCGAGGGAAGGAGTTCCGAGAGCGTGGACATGGCTTCTCCCACCTCCCCTGGCCCGGAGGG AGGGGCCTGCACCCCGCAGAACCCCCCGCGGATCCGTCAG
1´	ENSMUSE00001252380	127,409,058	127,408,845	-	-	214	GTCAGAGCAGATCATGTGGTGCTCTGTAGGCAGCTGGGACTGGCCCGCGGGAAGCACATGGATTACAGTCTGAGGCTGTGATGGGAAAGTCGGTTCCTGGGC TGCTGTCTCATACACATCAGCAGGCAGGGAAGCTGGGGACTCCGACTCGCCCTTCTCCGGGCCCCTCCTGCTGCGTGGTCACAGGCAATCGCTGAGAGAAGC TGCTGCTCCA
2´	ENSMUSE00001226003	127,339,192	127,339,132	-	0	61	GTAAGTAACTGATCAGGGACATGAAGAACTGCTATTTCAAATGACAACCATGTTGCAAAAG
3´	ENSMUSE00001237108	127,248,232	127,248,134	0	0	99	AGCCAAAACAAGTGTGAGAGCCAAACTACATGCAATGAAGTCACACAATCAAGCTGCATCCAACGCAAGGACCCCAATGGTGTGCATCCCGATGACCAG
1	ENSMUSE00001216415	127,225,932	127,225,764	-	0	169	GTCTCTTGTAAGTGCACGCACGCCAGTGGTCTGTTCCCGCGGCCGGGTTTGATGGCACAGCTATTTTCTTCCCAAACTGTTCAAAATGATGAACGAAGATGC AGCTCAGAAAAGCGACAGTGGAGAGAAGTTTAATGGCAGTAGTCAAAGAAGAAAAAGACCCAAGAAG
´1	ENSMUSE00001257111	127,162,342	127,161,679	-	0	664	TTTTCTCTCGCCCTGCATAGAGGTGTGGTTGCAAGCGGCAGAGAACTCCCCACCCCCCCTAGGACTTTCACCGAGGTGGCCTCTTCCTGGCTCCGGTCTGAA GACAGACTGTCTGGAGGAGTCCCCCAAGACCGTTCCAACTGGTGATGAGCGCCTAAGGAAGGCTTCTGCAACTATTAGGATGCTTGTCTGCACTCGGGGCCA CCCAACTGCTGAGGAGCTCCGGGTCCAGAGCTCCGCCCTCCCCCGGGACCATTGCTGAGCGTGGGCGCTCACCTGTGCATGCCTGTGTGCAGGTGTGGGCTG CTCAGGGGCTCGGCTCGCAACCTAGGGGGACGCTCGAGTGAATTATGGGTGCTGCAGAGGCTGGAGCAAGATTATGACCTAGCTCGGGGGCGGAGTGGATTA TTTTGTGAGTGTTCTGTCTGCCAGCCATTGCTCTGCTGGGGGGAAAAATCACATCTCCACATAGCAGTCAAATCACCTGTATTGCTGGGGAGTGGAAAGTTA TCCTCTGCCGATTTCGTCTGCCAAAATGGCTCACGCTGCTGCTTCTATCAAAAAAGTTAGAGAGGCTGAACTGGATGAAAAGGAAAAAAATCTGGACAGAGA GAGAAAAAAACAACGGAAAATCCCCAGGGATCGGATGGAGCGGAAAAGAAAG
2	ENSMUSE00001276722	127,104,862	127,104,761	0	0	102	TCTGACAGCAATGCCAGCTTCCTCCGCGCTGCCAGAGCAGGCAACCTGGACAAAGTGGTGGAATATCTGAAAGGGGGCATTGACATCAATACCTGCAATCAG
3	ENSMUSE00001294343	127,096,897	127,096,802	0	0	96	CAATGGAAGAGTAACCGATCCATGTGGACCAAGGAAACGAAGAGTCAGCTGGACGTGATAGTGCACGCCTTTAATCTCAGCATTTGGGAGACAGAG
4	ENSMUSE00001224175	127,079,996	127,079,898	0	0	99	AATGGACTCAATGCTCTCCACCTGGCAGCCAAGGAAGGCCATGTGGGCCTTGTGCAGGAGCTGCTGGGAAGAGGGTCCTCCGTGGATTCTGCCACCAAG
5	ENSMUSE00001293681	127,077,600	127,077,502	0	0	99	AAGGGAAATACCGCCCTTCACATTGCATCACTGGCTGGACAAGCAGAAGTTGTCAAAGTTCTAGTTAAGGAAGGAGCCAATATCAATGCCCAGTCGCAG
6	ENSMUSE00001288369	127,057,091	127,056,993	0	0	99	AATGGCTTCACTCCTTTGTACATGGCTGCCCAGGAGAATCACATTGATGTTGTAAAATATTTGCTAGAAAATGGAGCTAACCAGAGTACTGCTACAGAG
7	ENSMUSE00001297331	127,052,873	127,052,688	0	0	186	GACGGCTTTACTCCTCTGGCTGTGGCACTCCAACAGGGACACAACCAGGCGGTGGCCATCCTCTTGGAGAATGACACCAAAGGAAAGGTGAGGCTACCAGCC CTGCACATTGCTGCTCGGAAAGATGACACCAAGTCCGCCGCCCTCCTGCTTCAGAATGATCACAACGCTGATGTACAATCCAAG
8	ENSMUSE00001306055	127,052,249	127,052,226	0	0	24	ATGATGGTGAACAGGACAACAGAG
9	ENSMUSE00001295005	127,048,280	127,048,182	0	0	99	AGTGGCTTCACTCCTTTGCACATAGCTGCACACTATGGGAATGTAAATGTGGCAACTCTTCTTCTAAACCGGGGAGCTGCTGTGGACTTCACCGCCAGG
10	ENSMUSE00001220180	127,046,823	127,046,725	0	0	99	AATGGAATCACTCCTCTGCACGTGGCTTCCAAACGAGGAAATACCAACATGGTGAAGCTTCTACTGGATCGAGGTGGTCAGATTGATGCCAAAACTAGG
11	ENSMUSE00001234638	127,038,845	127,038,747	0	0	99	GACGGGCTGACACCACTTCACTGTGCTGCGCGGAGTGGGCATGATCAAGTGGTGGAGCTGCTGTTGGAACGGAAGGCTCCCTTGCTGGCGAGGACCAAG
12	ENSMUSE00001252274	127,032,313	127,032,116	0	0	198	AATGGGCTGTCCCCGCTTCACATGGCTGCGCAGGGGGACCACGTGGAATGTGTGAAGCACCTGCTCCAATACAAGGCGCCTGTCGATGACGTCACCCTGGAT TACCTGACGGCTCTTCATGTTGCTGCACACTGTGGGCACTACCGTGTAACCAAACTCCTGCTGGACAAGAGAGCCAACCCGAACGCAAGAGCCCTG
13	ENSMUSE00001235227	127,029,573	127,029,475	0	0	99	AATGGTTTTACTCCACTGCACATTGCCTGCAAGAAAAACCGCATCAAAGTCATGGAACTGCTGGTGAAATATGGGGCTTCAATCCAAGCTATAACAGAG
14	ENSMUSE00001267026	127,029,317	127,029,219	0	0	99	TCTGGCCTCACACCAATACATGTGGCTGCCTTCATGGGCCACTTGAACATTGTCCTCCTTCTGCTGCAGAACGGAGCCTCTCCAGATGTCACTAACATT
15	ENSMUSE00001300397	127,023,390	127,023,292	0	0	99	CGTGGTGAGACAGCTCTTCACATGGCGGCCCGGGCTGGGCAGGTGGAAGTGGTCCGATGTCTTCTGAGGAATGGTGCTCTTGTGGATGCCAGAGCCAGG
16	ENSMUSE00001255725	127,017,013	127,016,816	0	0	198	GAGGAGCAGACACCTTTACACATTGCCTCCAGGCTGGGGAAGACGGAAATTGTCCAGCTGCTTCTACAGCATATGGCTCACCCCGATGCAGCCACTACAAAT GGGTACACACCACTACACATCTCTGCTCGGGAAGGACAGGTAGACGTGGCCTCTGTCCTGCTGGAAGCGGGAGCAGCCCATTCCTTAGCGACCAAG
17	ENSMUSE00001261152	127,013,337	127,013,239	0	0	99	AAGGGCTTCACTCCCCTGCATGTAGCAGCCAAGTATGGAAGCCTGGATGTGGCAAAACTTCTCTTGCAACGTCGTGCAGCCGCAGATTCAGCAGGGAAG
18	ENSMUSE00001233123	127,012,771	127,012,673	0	0	99	AATGGCCTTACCCCGCTCCATGTTGCTGCTCATTATGACAACCAGAAGGTGGCGCTGTTGCTGCTGGAGAAGGGTGCTTCCCCTCATGCCACGGCCAAG
19	ENSMUSE00001263191	127,011,051	127,010,854	0	0	198	AATGGCTATACTCCCTTACACATTGCTGCCAAGAAGAATCAGATGCAGATAGCTTCCACACTACTGAACTATGGGGCCGAGACTAACACTGTGACAAAGCAA GGGGTCACTCCACTGCATCTGGCCTCACAAGAGGGGCACACAGACATGGTCACCTTGCTTCTGGACAAAGGAGCCAATATCCACATGTCAACCAAG
20	ENSMUSE00001253269	127,004,043	127,003,945	0	0	99	AGTGGACTCACATCCTTACACCTTGCAGCCCAAGAAGATAAGGTGAACGTTGCGGACATTCTCACCAAACACGGGGCCGATCGGGATGCCTACACAAAG
21	ENSMUSE00001233506	127,002,776	127,002,678	0	0	99	CTTGGTTACACACCTTTGATCGTGGCCTGTCACTATGGAAATGTGAAAATGGTCAACTTTCTTCTGAAACAGGGAGCAAATGTCAATGCGAAAACCAAG
22	ENSMUSE00001232182	126,998,975	126,998,877	0	0	99	AATGGCTACACACCTTTGCACCAAGCTGCCCAGCAGGGCCACACACACATCATTAATGTCCTGCTCCAGCACGGGGCCAAGCCTAATGCTACTACTGCG
1s	ENSMUSE00000669796	126,998,461	126,998,324	-	-	138	AGTGTCCTGGGCTGGATGCAGCCAGAATTGCTAGCTTGTATAGTTTGTGCAGCACTGGAGATCCTGCAGCGCAGAAGCTAAATCTGTCACTGGGTCCCTATG GTAACATCTTACCTGCAGCAGATGGCCTGACTCTTG
23	ENSMUSE00001307115	126,997,951	126,997,853	0 -	0 -	99	AATGGTAACACGGCCCTGGCGATTGCTAAGCGGCTGGGCTACATCTCCGTGGTTGACACCCTGAAGGTTGTGACTGAAGAGGTCACCACCACTACCACG
24	ENSMUSE00001285026	126,988,216	126,988,144	0 -	1	73	ACTATCACGGAAAAACATAAGCTAAATGTTCCTGAGACAATGACGGAGGTCCTTGATGTTTCTGATGAAGAGG
25	ENSMUSE00001275399	126,981,944	126,981,800	1	2	145	GTGATGACACTGTGACAGGTGATGGGGGAGAATACCTCAGGCCAGAAGATCTCAAGGAGCTCGGAGATGACTCACTGCCCAGCAGTCAGTTCCTGGATGGCA TGAACTACCTTCGGTACAGTCTGGAGGGAGGAAGATCCGACAG

26a 26b	ENSMUSE00001274268 n/a	126,976,947 126,976,932	126,976,845	2	0	103 88	CCTCCGGTCCTTCAGTTCCGACAGGTCTCACACTCTGAGCCATGCATCGTACCTGAGGGACAGTGCCATGATTGACGACACGGTTGTGATCCCCAGCCACCAG
27	ENSMUSE00001304535	126,976,154	126,976,051	0	2	104	GTGTCTGCGCTAGCCAAGGAGGCAGAAAGGAATTCTTATCGTCTGAGCTGGGGCACTGAGAACTTAGACAACGTGGCTCTTTCTTCCAGTCCTATTCATTCAGG
28	ENSMUSE00001285906	126,971,038	126,971,003	2	2	36	CCGCTCCTCTCCATGTCTCGATCGTGACAACAGCAG
29	ENSMUSE00001288521	126,965,162	126,964,938	2	2	225	TTTCCTAGTCAGTTTTATGGTGGATGCCCGTGGTGGTGCCATGCGAGGATGCAGACACAATGGACTCAGAATCATTATCCCACCTCGGAAATGCACAGCCCCAACTCGCGTCACCTGCCGCCTTGTGAAACGCCATCGACTGGCAACAATGCCGCCCATGGTGGAAGGAGAAGGCCTGGCCAGCCGCCTGATTGAAGTCGGACCTTCGGGAGCTCAGTTTCTTGG
30	ENSMUSE00001222661	126,963,481	126,963,383	2	2	99	TAAACTTCACCTGCCAACGGCTCCTCCCCCACTTAATGAGGGAGAAAGTTTGGTCAGCCGCATCCTTCAGCTGGGGCCTCCTGGAACCAAATTCCTTGG
31	ENSMUSE00001233359	126,962,405	126,962,251	2	1	155	GCCCGTGATCGTGGAGATCCCTCACTTCGCCGCTCTTCGAGGAAAGGAGAGGGAGCTGGTGGTCCTGCGCAGTGAAAATGGGGACAGCTGGAAAGAGCATTTCTGCGACTACACTGAGGATGAATTGAACGAAATCCTTAATGGCATGGATGAAG
32	ENSMUSE00001268007	126,959,864	126,959,653	1	0	212	TGCTGGACAGTCCAGAAGACCTGGAAAAGAAACGAATCTGCCGCATCATCACTCGTGACTTCCCACAGTACTTTGCGGTGGTGTCTCGCATCAAACAGGACAGCAACCTGATTGGCCCCGAGGGTGGAGTACTGAGCAGCACAGTGGTGTCACAGGTGCAAGCCGTCTTCCCAGAGGGCGCACTCACCAAGCGCATTCGAGTAGGCCTACAG
33	ENSMUSE00001227835	126,959,087	126,958,883	0	1	205	GCTCAACCTATGCATAGTGAATTGGTAAAGAAGATCTTAGGCAACAAAGCCACCTTCAGCCCAATAGTCACTTTGGAACCCAGGAGAAGAAAATTCCACAAGCCAATTACTATGACTATTCCTGTCCCCAAAGCTTCAAGTGATGTCATGCTGAATGGTTTTGGGGGAGACGCACCAACCTTAAGATTACTGTGCAGCATAACAG
34	ENSMUSE00001297707	126,957,352	126,957,256	1	2	97	GTGGAACTACGCCTGCCCAGTGGGAAGACATCACAGGAACAACGCCACTAACATTTGTCAATGAGTGTGTTTCCTTTACAACCAACGTGTCTGCCAG
35	ENSMUSE00001287914	126,956,098	126,955,870	2	0	229	GTTCTGGCTGATAGACTGTCGACAGATTCAGGAGTCTGTTGCCTTTGCATCACAAGTGTATAGAGAAATTATCTGTGTGCCATATATGGCCAAATTTGTAGTGTTTGCCAAGTCACATGACCCCATTGAAGCCAGGTTGCGGTGTTTCTGTATGACAGATGACAAAGTAGATAAGACCCTTGAACAACAAGAAAACTTCTCTGAGGGTGGCCAGGAGCAGGGATGTGGAG
36	ENSMUSE00001233894	126,955,109	126,954,984	0	0	126	GTATTGGAAGGAAAACCTATTTATGTTGATTGTTTTGGCAACCTGGTTCCACTAACCAAGAGTGGCCAACATCATATATTCAGCTTTTTTGCCTTCAAAGAAAATAGACTTCCTCTCTTTGTCAAG
37	ENSMUSE00001249776	126,953,299	126,953,177	0	0	123	GTTCGTGACACAACCCAGGAACCTTGCGGGCGACTCTCATTTATGAAGGAACCCAAATCCACAAGAGGACTGGTGCATCAAGCTATTTGCAACTTAAACATCACCCTGCCAATTTATGCCAAG
38	ENSMUSE00001281374	126,952,521	126,952,489	0	0	33	GAATCGGAGTCAGATCAAGAGCCGGAGGAAGAG
39	ENSMUSE00000669794	126,950,756	126,950,735	0	1	22	ATCGGTATGACATCCGAAAAAA
40	ENSMUSE00001250226	126,947,807	126,941,610	1	1	6198	ATGATGAGACAGAGTCGACAGAAACATCTGTCCTGAAAAGCCACCTGGTTAATGAAGTTCCTGTCTTAGCAAGTCCGGACTTGCTCTCTGAAGTTTCTGAGATGAAACAAGATTTGATCAAAATGACGGCCATCTTGACCACAGATGTGTCTGATAAGGCAGGTTCGCTCAAAGTGAAGGAGCTGGCAAAGGCCGGTGAAGAAGAGCCAGGCGAGCCCTTTGAAATTGTAGAGAGAGTGAAGGAGGACTTAGAGAAGGTGAATGCGATCCTGAGGAGTGGAACATGCATGAGAGATGAAGGCAGAGCGCGGAGTTCTCAGTCTGAGCGGGAGCTAGAGGAGGAATGGGTTATTGTCAGCGATGAGGAAATCCAAGAGGCCAAGCAACACGCCCCAGTAGAAATCGATGAACACCCATGTATAGAGGTCAGAGTAGACAGAGAGACCAAGGCCAAAGTAGAAAAGGACTCTACTGGGTTAGTGAACTACCTCACAGATGACCTAAATTCATACACTAGTCCTCATGAAAAGAAGCCACACACAGCTCCAGAAAAGTCAGGGGAGACAAGTCAGGCTTCAGCTGTTGGCAAGAGCTCTGAGAGTAATAAGGGGAAGGCCACCTCAGCCGAGGAGAAACAGAGCGCTCAGAAGCAGCTCAAACCAGGCCTGGCGATCAAAAAGCCAGTGAGGAGGAAACTAAAAGAGAAGCAGAAACAGAAAGAGGAAAGCTCGCAAAGCAGCGAAGAAAAGACCGAACTTAAGAAAGGTAGTTCAGAGGAGTCGGTAGATGAAGACCGCGGCCTGGTCCCTGAACCCCTCCCCACTGCCAAGGCCACCTCTCCTCTCATAGAAGAAACTCCTATTGGTTCCATAAAGGACAAAGTGAAGGCTCTTCAGAAGCGAGTGGAAGATGAGCAGAAAGGCCGAAGCAAGCTGCCAGTCAGAGTCAAAGGCAAAGAGGATGTGCCCAAAAGGACCACTCCCAGGACACACCCAGCTGTGTCACCCTCTTCAAAGTCATCGACTTCCTCTAAAGCAGAAAGACACTCTTCCCTTTCTTCCTCCGCAAAACCTGAAAGGCACACACCAGTGTCACCGTCCAGCAAAAACGAAAAACTCTCACCTGTGTCACCCTCGGCCAAAACCGAACGGCATTCACCAGTATTTTCAGGTAAACCCGAGAAACACTCACCTGGTTCCCCCTCAACCAAAAATGAAAGACATTCCCCTGTGTCATCTCTAAAAACAGAACGACACACACCCGGGTCCCCTTCAGGTAAGACAGACAAACGTCCACCGGTGCCATCATCTGGAAGAACAGAGAAACATCCCCCAGTGTCACCTGGCAAAACCGAAAAACACTTGCCCGGTTCCCCTTCTATAAGAACCCCAGAGAAGCCGGCACCTGGGTCTGCCACCGGGAAACATGAGAAGCACCTCCCTGTGTCTCCTGGGAAGACAGAAAAGCAGCCACCCATATCTCCCACCTCCAAAACCGAACGAATTGAGGAGACAATGTCTGTCCGGGAGCTCATGAAAGCATTCCAGTCAGGTCAGGACCCATCTAAACACAAAACAGGACTCTTTGAGCACAAGTCAGCCAAACAAAAACAGCCGCAAGACAAAAGTAAAAGTCGGGTAGAAAAAGAAAAAGGGCACACTGTGACCCAGAGAGAAACACAGAGAATAGAAAGTCAGACAGCCAAGCGTGGCCAGAGATTCCAGGTCTCGGCAGCTACGGAATCCAGAAGGTTCCGTTCTACCACCATCACCGTTGGGCTCAGGATGGAAGATCCAGTTAGAGAAAGGTTTGAGAGAACCCCCATTATTAAAACACCCGAGGTAGTTCCATCAGTGGCGGCAGAAGAGAGCCATCGTGGGAGTGAGAAGATTGTGGATGAGCAGGGAGACATGGACTTCCAGATCAGTCCAGACAGGAAAACCTCCACTGACTTTTCTGAAGTCATCAAGCAAGAGTTAGAAGACAATGACAAATACCAACAATTCCGCCTCACCGAGGACACAGAAAAGGCTCAGGTTCATTTAGACCAAGTAATTACGAGTCCCTTCAACACGGCTTTCCCACTAGATTATATGAAAGACGAGTTCCTTCCAGCTCTGTCTTTACAGAGCGGTGCTTTGGGTGGCAGTTCCGAAAGCCTGAAACAAGAAGTGATAGCAGGCTCGCCTTGCAGCAGCCTGATGGAAGGCACGCCTCAGATCAGTTCAGAAGAGAGCTACAAACATGAGGGCCTAGCAGAAACTCCTGAGACAAGTCCAGAGAGTCTTTCTTTCTCACCAAAGAAAAGTGAGGAACAGATTGGAGAGGCTAAGGAAACTACCAAGGTAGGAACACCCACAGACATTCATTCAGAAAAAGAGCTTCCTATAACTAATGACATTACTGATAGTTCTCAAAAACAAGGTGCTGGGGTCACTCGGGGTTCAGAGCCCTCTACAGAGCATTCTCAGAAGGAGGTCACCCAAGACCCTCACAAAGATGTGTGCTCCAAACAAGATGGCTGCCCTGAGAGCCAGAGTGTATCATTAGCAAGTGAGGTGTTTACTGAGAAAGGGTCCTGTGGTGAAAGTCAGCTTCCACTTGTTAGCTCAGCTTTTAAGACACAATCAGAAAGTGAAACTCAGGAATCCTTAACACCCTCAGAAGTGACAAAGCCCTTCCCACCATCTGATGCTTCCGTCAAGACAGCTGAGGGAACTGAACCAAAGCCCCAGGGAGCTATTAGAAGTCCCCAAGGGCTAGAACTTCCTCTCCCTAACCGGGATAGTGAGGTCCTTAGCCCAATGGCTGATGAATCATTAGCAGTCAGCCACAAAGACTCTCTGGAAGCCAGCCCCGTGCTAGAAGATAACTCCTCCCACAAAACCCCTGATTCTCTGGAACCAAGTCCTCTGAAAGAGTCCCCTTGCAGGGACTCCCTTGAAAGCAGCCCGGTTGAGCCTAAAATGAAGGCAGGAATACTCCCAAGTCACTTTCCCCTCCCCGCAGCTATTGCCAAAACAGATCTTGTTGCGGAAGTGGCCTCCATGCGTTCCCGGCTGCTCCGAGACCCCGATGGCAGTGCTGAGGATGACAGTCTAGAGCAGACATCCCTCATGGAGAGCTCAGGGAAAAGCCCCCTGTCCCCTGACACCCCCAGCTCCGAGGAAGTTAGCTACGAGGTCACACCCAAACCTTCCGATTCAAGTACACCCAAACCGGCTGTGATTCACGAATGTGCAGAAGAGGATGACTCTGAGAACGGGGAGAAGAAGAGGTTCACGCCAGAAGAGGAAATGTTCAAAATGGTAACCAAAATTAAAACGTTTGATGAACTTGAGCAAGAAGCAAAGCAGAAAAGGGACT

							ACAAAAAAGAACCCAGGCAAGATGGGTCCTCCTCAGCCTCGGACCCCGATGCTGACTATTCAGCAGAAGTGAATGACGAGAAACAGATGGCGGGCACAGAGG GGGAGGGGGAGGTCCCTGTCTTGGTGACTTCAGAGAACAGAAAGGTTTCTTCTTCCTCCTCGGAGAGCGAACCTGAGCTGACACAGCTGAGTAAAGGTGCTG ACTCGGGACTTCTGACGGAGCCAGTTATCCGAGTGCAACCCCCATCTCCCCTCCCATCCAGCATAGACTCTAATTCTAGCCCCGAAGAAGCAACGCAGTTCC AGCCCATAGTTCCCAAGCAATACACTTTCAAGATGAATGAGGAGATTCAAGAAGAGCCAGCTACTTCAGAAGATAAAGACTGCAAATCACATTTAGCGGAAG ACAGTCAGACTCATTCTGCTGATGCTGCTGATGGGTCTGATGGTGACCTGAACAGAGAGACTACTCAGCCAGAGACCTGTGATGGCCATGGTTGTGAGACTG TGAGTCCTAGCAACTCAGCCACTCCTGTCTCCCTAGGAGTTCAGAGTCCAGAGCATAAAGATGTCGATAAGCCCCTGGCCATTGATAAAGACTCACTAGCTC ACCAAGATACTTGTGAAAATGACCGAGAAGAAAGAGAGTTTGATCCTTCTGGAGTAGAATCTACTCAAGCAGATCTTCCCAATGAAAGCTCTTCCTTGTCTT CTCGTTGTGCGATACCTGAAGGAAATGAATCAGCTAAAGAAATAGCCTCTCCATCTTCCCCTGTAAAAGTAGAGGTCACGATAACTGACCAGGCTTTGGAGA GCATGCCAGAGGACTGTCCCATTCAAGACTCATCTACTACAATGCAAACAGAGAGGTTTGCCATGGACGTTCCAGTGTCTGAGTTAGCTGAGACTGATGAAA ATTCTGACCCTCAAATCATCAGCCCTTATGAAAATGTTCCTTCCTCATCGTTCTTCTCTGCTGAGCCCAGCAAAATCCAAACAGATACCTGTCATAGCACAG TTGTTCATTCACCTGAAGTGTATTCTGTCATCATCAGATCCTCTCCTGAGGATGTGGTAGTGACAAACTCCTCTAACAGAACTGTCTCAGGTGAAGAGTCTC ATTGTGAGAGCCACGATCTAGAAACTGAATCCGAGCAAAAAAGTGCTTTGTGGGCCGCGCAGTCTGATGCACCTCCCTTGGCCGTAGCACCCACCGCATCAG ATGCAGCATCAGTCACTGGGGAACAAGCAAGCAAAGTCATCATCACCAAAACGGATGCTGATGCTGACTCCTGGAGCGAGATCCGTGAAGACGACGCAGCCT TCGAAGCTCGGGTGAAGGAGGAAGAACAGAAGATATTCGGTTTGATGGTAGACAGGCAGTCACAGGGCACCACTCCTGATACCACTCCTGCTAGGACCCCAA CTGAAGAGGGGACTCCGACAAGTGAACAAAATCCATTCCTCTTTCAGGAAGGAAAACTGTTTGAGATGACCCGAAGTGGTGCTATCGATATGACCAAAAGGC CCTATGCAGATGAAAGTTTGCACTTTTTCCAAATCGGCCAAGAGTCCAATGAAGAGGCTATCTCCGAAGACTTGAAGGAAGGGGCCACTGGGGCTGAGCCTC CACAGACGGAGACTACTAGTGAGTCGCTGGAACTTTCAGAACCCAAAGAAGCAATGGATGACGAAGGAGAATTACTTCCTGATGATGTAAGTGAGGAGATAG AGGATTTACCTGCCTCGGATGCTAACATTGACTCCCAAGTGATAATTTCAGCTTCCACAGAAACACCCACCAAAGAGGCTGTATCCACAGCGGTCGAGGAGC CCCCCACCACACAGCGGAGTGATTCTCTGAGCACTGTGAAGCAGACACCACGCCCTGCCGTCCCTGGACCTGTTGGTCAGTTGGACTTTTCCCCCGTCACTA GGTCTGTTTATTCGGGACAGGATGATGAGTCCCCAGAGTCTTCTCCAGAGGAACAGAAGTCTGTGATTGAGATCCCTACTGCACCCGTGGACAACGTGCCTT CTGCCGAAAGCAAACCCCAAATTCCTATCAGGACTCTCCCCACTTTAGTCCCAGCCCCTCCATCTGCAGAGGATGAGAGTGCATTTTCTGATGATTTCCCAT CTAGCCTGGATGAGGATAGTAAGGAAGGTGGAGCAAAACCAAAGTCCAAAATTCCCGTCAAAGCACCCACCCAAAGAACTGAGTGGCAGCCCTCCCCTACCG ACATACCTCTCCAGAAGACAGCTGTCCCCCAGGGACAGGAAACACTAAGCAGAGCACCAGATGGTAGAAGCAAGTCAGAGTCAGACGCTAGTTCCTTAGATG CTAAGACCAAATGCCCAGTGAAAGCCAGAAGTTACATTGAGACAGAGACGGAGAGCAGGGAGAGGGCCGAGGGGTTTGAGTCAGAATCAGAAGACGGGGCCA CAAAACCAAAGCTCTTTGCATCCCGACTGCCGGTGAAGAGCAGGAGCACTTCATCTTCCGGCAGGCCAGGCACGAGCCCCACCAGAGAGAGCAGGGAGCACT TCTTTGACCTTTACCGAAACTCCATAGAATTCTTTGAGGAGATTAGTGATGAAGCTTCCAAATTAGTGGACAGGCTTACACAGTCAGAGAGGGAGCAGGAGC CACCTTCAGACGACGAAAGTAGCAGTGCCCTGGAAGTGTCAGTCATTGAGAGTCTGCCACCTGTTGACATTGAGCACTCAGCTCCCGAGGACATCTTTGACA CAAGGCCCATTTGGGATGAGTCTATTGAGACTATGATTGAACGCATCCCTGATGAAAATGGCCATGACCGAGCTGAAG
41	ENSMUSE00000563439	126,940,146	126,940,072	1	1	75	ATCCCCAAGATGAGCAGGAGCGGATGGAAGAAAGGCTGGCTTACATCGCTGATCACCTTGGCTTCAGCTGGACAG
42	ENSMUSE00000563435	126,937,869	126,937,738	1	1	132	AATTAGCAAGAGAACTGGATTTCACTGAGGAGCAAATTCACCAAATTCGAATCGAGAACCCCAACTCCCTTCAAGATCAGAGCCACGCACTGCTCAAGTACT GGCTGGAGAGGGATGGGAAGCATGCCACAG
43	ENSMUSE00000563434	126,936,763	126,936,620	1	1	144	ATACCATCCTCATCGAATGCCTCACCAAGATCAACAGGATGGACATTGTACATCTCCTGGAGACCAACACAGAGCCCCTCCAGGAGCGCATGGGCCGCAGCT ATGCAGAAATAGAGCAGACCATTACGCTGGACCACAGTGAAG
44	ENSMUSE00000563431	126,934,778	126,934,526	1	2	253	GATTTTCAGTCCTTCCAGACGAGCTCTGTGCTGCCAAGGAGAAGAAGGAGCAGGAAGCTTCCAAAGAAAGCGAGTCTAGCGACCACCCGCCCATGGTCTCCG AAGAAGACATATCTGTCGGTTATTCCACATTTCAGGATTGCCTCCCCAAAACTGAAGGGGACAGCCCAGCAGCAGCACTGTCTCCTCAAATGCACCAGGAGC CAGTTCAACAAGATTTCTCAGGGAAAACGCAAGACCAGCAGGAATATTA
45	ENSMUSE00000563429	126,933,226	126,932,938	2	0	289	TGTAACAACACCAGGGGCAGAAGTGGAAGACCCTCAGAAGGCCACAGCCGTTCCTGACTCTCTCTGTAAGACTCCTGAGGACATCAGTACCCCTCCTGAGGG AACAAAGCCTTGTCTCCAGACCCCGGTGACTAGCGAACGTGGTTCTCCGATTGTGCAAGAACCTGAGGAGGCTTCCGAGCCCAAAGAGGAGAGTTCTCCAAG GAAAACTAGCCTGGTCATTGTTGAGTCAACAGACGACCAGTCTCAGGTCTTTGAAAGACTGGATGGTGATGCCGCTTTTCAAAAG
46	ENSMUSE00001260738	126,930,653	126,930,561	0	0	93	GAGCTAACAGAGGAATTAGGAGAGCTGGAGGCTAGCTCTGATGAGGAGGCCATGGTAACTACCAGGGTTGTCCGCCGGAGAGTGATTATCCAG
47	ENSMUSE00000563426	126,930,081	126,929,998	0	0	84	GGAGACGATATGCCTGACATACCCCCAGAGACGGTCACAGAGGAAGAATATGTTGATGAGAATGGACACACCGTGGTGAAGAAG
48	ENSMUSE00001081872	126,929,886	126,929,722	0	0	165	GTTACCCGGAAAATCATTAGGCGGTACGTTTCCTCTGATGGCACAGAGAAGGAGGAGGTTACCATGCAGGGAATGCCTCAGGAGCCAGTCAACATTGAGGAT GGGGACAATTATTCCAAAGTGATAAAGCGCGTGGTATTGAAGAGTGACACCCAGCAGTCAGAG
49	ENSMUSE00001077693	126,928,847	126,928,665	0	0	183	GTGACTTTGTCTGAACCCAGCGTTTTGTCCAGTACCTCACAGTTTCAGGCCGAGCCAGTAGAAGGCCGTAGAGTCAGCAAAGTTGTTAAAACAACCATGGTA CACGGAGAACGGATGGAGAAGAGTCTTGGGGACTCTAGCTTAGCCACTGACCTTCCTTCAGCCAAAGATGACTTTGAAGAG
50	ENSMUSE00001303914	126,926,894	126,926,803	0	2	92	GCTTTGGGGTACACAGGTAGCCATATGAACGTCCACTTGCCCAGTTTAGTAGAGAATGAAATCCTGAAGGAGGATGGATCAATAATTAAGAG
51	ENSMUSE00001243556	126,923,971	126,921,606	0	-	2366	GACAACAATGAGTAAAGCCAGGACACAGAGGAGGGCTGTGGTGAAGGACCAGCAGGGGAAACACATCACCTTGGAGCACCTGGAGGATGTTCCCGGAGCACT GGACCAAGACGACCTCCAGCGAGATCTCCAGCAACTCCTTCGGCACTTCTGCAAGGAGAACACAAAGCAAGAGGCCAAATGAGGAGCTGCCCAGTTCTCACC AGAAACCACAAACCCACTCAATATGCAACTTCCCATTTCTGCGCAGGAGTGACTGAAGTGGCCTAATTACTGGGACCCAGTGACACTTCCACTCTCAGCAAA CACACAGCATCTACTTTTCCTTCTTTCTCCCTGCCCCTCTCTAACTATAAGCTAATTTGTGACCAAAGATAGCATCCTTCCTTCCGGATGCTGTATCCACTA TTTTGAGCATCCGTGCTAACCTGGGAACTGGCATCTCTATTGTTTGCTTCTGCTCAAGCTCCATGAAACTCCATGAATCAGAAGAACTTCACCTGCAGACTT CTTCAAATGACAGGGGAATCCTTCCAAGGGTATCTATGTATAATGTATATAGCCGAAATTCTCAGACGAACAACAGAGTAAAATTCAAACCACTGCCTGTCA TAATTACACTGGGCATCATGGAATAAAAGCCTCTAGATATTGCTGAACAATGGTTAATTATGATATTGCTAACACAATCAAATGGTAATACAGTTCTATGGA AGAAACACTTCAGACTTAGACACGTCCTTAGAACTTCCAGAGTAGCCATTTGCTCTTAAAGCCGTCAGGATCATAATCTTGAAGAAGAATCCCTAGGAGTGG TCTCTAGGACTGGTCAGCCATAGCCGTTGGCTCTTGGACTGTGGCCCTGAGGGAGAGGGAGAAGGACTCACAGGCCAGCAGATGGAAACAGCGAGGTATTCT GGTGCTAGAAGCTTCAGGGGTGGTGTTCTAGCACCTTCAGGTGTTTTTGACTTTGGACACGTTGGCAGGGTATTTTAAAAGCTATAACTACTGTAGTTTTCC GGTGTTCATTGCTGCTTTAGCAAACCACGCTGTCTTACTGGTGGTACTTTCTTCTGGCCACTGCACTGTAGATAATTCATTGGAAACAAGATTTATGCACCA CACAAAAGGTTAAATGCTGTCACCATGTTGGAGTGGTTTCTTTTCTTTTCTTTTCTTTTCTTTTCTTTTCTTTTTCCCCACCTCCAAGTTTA TCTTTCCTCTAATACCTGCATGTAGCATCACACACACACACACACACACACACACACACACACACACACACACACACATCTTCTCATTACACTAATGGTTTTCACT CTGAGTCTCAACTTTCTCGCCATGTCTGCTCTTCAGCTTGCAGATGAGATTTTGGGAAATCCTTGGAAAATTTGGTTCTCATTAATTTTTTTTTTTGGTTTA TTTATTCAAACCCCAGTCACTCTTGGAAACTGAAGTGCATTTGTGTGACTTTCTGTTTGTTTTAGAGAAGGGACAATGACAGTCTGAGTGCTCCCCATGCCC

							TATGTCGAATCCCCCTAGTGATTGAAGCTGTGTAGCATTTTAACATATATATATAAATATATTCACAAATATATTCATATAAACAGTATACGTTTTGAATCA GTTATTTGTTAAAGAAAGTATATTCAATGAAGATGAAATTAAAAAGAAAAAGAAAGAAAGAGAGAAAGAAAGAAAGAGAGAGAGAGAAAGAAGGAAAACAGC CTACCCTCCAGAGACTGACATTTTTCCAGTCCTATCTAGCCTTTTCCTGTGTGCAGAACTGACTCATTGCTCGGAATGTCAGACACAAACACGACAAACAAT AGCACTTCATCTTTTTGAGTAACATTGCCAAGAGAAGAATTTTCCTGGGAGAGAGGTTTCCCATCAGGCAAATCTCCTGAGTCCCCGGCACTAGCACTTTCT GGGGGACTGTGTAGAAACAAAGTGTTCTTTGGCATCCAAACTGAGAGAGAGAGGCAGGTGGCAGCCCTTCTTGAGATATGAGGTGGCCATCTTATCAGATCT TTGCCCTGGAGCTCATGAAAAGCCTTTCTGTTGTGTTATTTGCAGTGCAGATGATGTCCTTGTGGCAACTTAATGGTTCTTCACTTTTTTTTCCTTCAATTT TAATTTTTTTTTTTTTTTGCTGTGTTATCAAAAACTTGAATACTGTGAGAAGTGAATTTTCAGTTGATGAATCAGCATCTTGTTCCCATGGTGATAACACTAA TTGAATATATCTATGAGGGCATGTATTAGTTATTGGAAAACAATACAACACTAACAATACATAGCTGCAATGTTGTACAATGGCTGATTTAACTAAATAAAA TGTATAAGTGTTAAGTGTTG

Exon No.		Start	End	Start Phase	End Phase	Length	Sequence
1a	n/a	69,398,773	69,399,129	-	0	357	GTTGTCTGGGGGACCCTGCGGCGGACAGCACTGGGCATGCTCGGGCGGCAGTGGGCCGGGCGGGTCGCCGCGCCTCCACCTGGCTGTCCCGCCCCCCGCAAGCCA ACCGAGCAGCACCTGGCGGCGCCCGGCAGGGGGAGGAGAAGGCGCGGGGCGGCGCTGCGCGTTCCCGAGCCGTGGCCCAACTTTCACCCCCACTTTCCCTCCTGG GGGTGCAGTCCCTGGATCGGGGGTTGAGGAGACGCCGACTCGAGCGCAGAGCCGAGTTCCTGGAAGGCGGAGCGCGCGAGTACCCACCGTATGGCCTGCTCGGG CACCTCGTCCCCAGTGGGCGCGGGGAGCCCCGATCTTGAGCAG
2a	n/a	69,484,229	69,484,267	0	0	39	GGTGACTTTGGATCCTGTTATTCACGAAGCTCTCAAAAG
1e	ENSMUSE00001241754	69,533,772	69,534,284	-	0	513	GTGTGTGTGTGTGCAGCGCACATGCACGTATGCCTCCCCCTTTCTCTCTCTCACCATTTCCAAGCTAGAATCACCGTGGAGAAGCAAGCCCTGAAATGTTGTCAA GATCTTTTCTCGGGGTAACGACTGGCTAAAAAAACAAATAAAAAGAGAGAGAAAGGAAGAAAAAGAAAGAAGGAAGAAAGGAAGGAAGAAAACAAAGGGTTGGAA TATTGATTTTTCTTTGGAGGAATAACCAGGGCTTTGCTGGAGAGAACACCCAGTTCCTCCCTGAGGCGAGCTGAGTTGCCCGTGACAGCAGCCAGGGCTGGCTTG AAGCAGCCGCTCTGCCTGGGGAGTTCCCTAAATGGACTTTGGTCTCAATGCTGTGACTCTTTGCCGTGGGTTTGGATGTGGGAACACGGAAGGTGATCTCCTGCC TCGTCTCAACTCCCCTGATCTCAAGGAAAGATGAGTGAAGAGCCAAAGGAGAAGCCCGCCAAGCCTGCTCATAGGAAGAGGAAAGGAAAAAAG
1b	ENSMUSE00001240581	69,706,370	69,706,925	-	0	556	AGGATTAGTGCTGGCTTCTCGGCTGCCGCATGTGGGGTGACTCCGGATCTTTCTCCTTTACAAGAGCCACCCTTTGCAGCATTCCCCCTTTGGAGGAACCACTTA GACACTTCCAGCTAGTGGCAGGGGATGCGGCCATAACACAGCTCCTCCGGTCCCAGCTGCCTCCACTACAGCCTCTGCACCAGGATGGCTGTGCTCTCCTCCAGA GGGGAAGGCTCAGCAAGGTGTAGGATGAGATCTGGCCCCTGCTGTGGTGGGTTTTGAAAGCTGCAGTTTCCCCAGCATCTCTGCCTCTCTGCCTCTTGGATGCCT TTCTGCTCAGGCTTCTCTCCTGCGAGGGCTATGCTGCTCTATGCCTGATTAGAGGTACCCAAGGAGATCACCTTTCTCAGAGAAAGCTCTGCGCGCTGCTTGAGA CAGGGTCTTTTTCAAATGCATTATGGCTCATGCCGCCTCCCAGTTAAAGAAAAACAGGGATTTAGAAATCAATGCGGAAGAAGAGACTGAGAAAAAAAGGAAAC ACCGCAAACGGTCCCGGGATCGCAAGAAAAAG
1f	ENSMUSE00001263979	69,785,525	69,785,672	-	0	148	AGGAGGTCGGGGAGACGTCTTTACGTTTTCCAAGGCGGATATTTTTAGACAGGATGTTCTGCCCCAAGTGTTAACTAATTGAGTTATCAGGTTTCGTATTTGGCC TCAGAGAATGGCCGTGGAAGAGCCAGAGGGCTTCCCAGAAGAA
2	ENSMUSE00001282033	69,808,416	69,808,517	0	0	102	TCTGATGCCAACGCAAGTTACTTAAGAGCAGCTCGGGCAGGGCACCTGGAAAAGGCCCTTGACTACATCAAAAATGGAGTGGACGTCAACATCTGTAACCAG
3	ENSMUSE00001280093	69,808,873	69,808,971	0	0	99	AATGGATTGAATGCACTCCATCTTGCTTCCAAAGAAGGCCATGTGGAAGTGGTCTCTGAGCTGCTGCAGAGGGAAGCCAATGTTGATGCCGCCACAAAG
4	ENSMUSE00001274976	69,809,171	69,809,269	0	0	99	AAAGGAAACACGGCCTTACACATCGCATCTTTGGCTGGGCAAGCGGAAGTGGTCAAGGTCTTGGTTACGAACGGAGCGAATGTCAACGCACAATCTCAG
5	ENSMUSE00001241373	69,815,695	69,815,793	0	0	99	AATGGCTTCACACCATTGTATATGGCAGCCCAGGAGAACCACCTGGAAGTCGTCAGGTTTCTTCTGGACAATGGCGCCAGCCAAAGCCTGGCCACAGAG
6	ENSMUSE00001288955	69,822,208	69,822,393	0	0	186	GACGGCTTCACGCCATTGGCCGTGGCTCTGCAACAAGGTCATGACCAAGTCGTGTCCCTCCTGCTCGAGAACGACACGAAGGGAAAAGTGCGCCTCCCAGCCCTC CACATCGCAGCCCGGAAAGACGACACCAAGGCAGCAGCTCTGCTCCTGCAGAATGACACAAACGCGGACGTGGAGTCAAAG
7	ENSMUSE00001258555	69,823,078	69,823,101	0	0	24	ATGGTGGTGAATAGAGCAACTGAG
8	ENSMUSE00001214460	69,824,318	69,824,416	0	0	99	AGTGGCTTCACCCCGCTCCACATAGCTGCCCACTATGGGAACATCAATGTGGCCACGTTGCTGTTAAACCGAGCGGCTGCTGTGGACTTCACCGCACGG
9	ENSMUSE00001258730	69,850,106	69,850,204	0	0	99	AATGACATCACTCCCTTACACGTTGCCTCGAAGCGAGGAAATGCAAATATGGTGAAGCTATTGCTGGACCGGGGTGCGAAGATCGATGCCAAGACCAGG
10	ENSMUSE00001250647	69,867,385	69,867,483	0	0	99	GACGGTCTGACTCCGTTGCACTGTGGGGCGAGAAGTGGCCATGAGCAGGTGGTAGAGATGTTGCTTGACAGATCCGCCCCCATCCTTTCAAAAACCAAG
11	ENSMUSE00001297249	69,871,002	69,871,199	0	0	198	AATGGATTGTCGCCACTGCACATGGCCACACAAGGAGACCATTTAAACTGCGTCCAACTCCTCCTCCAGCACAACGTGCCCGTGGACGACGTCACCAACGACTAC CTGACTGCCCTCCATGTGGCTGCCCACTGCGGCCATTACAAAGTTGCCAAGGTTCTTTTGGATAAGAAAGCTAGCCCCAATGCCAAAGCCCTG
12	ENSMUSE00001307807	69,874,790	69,874,888	0	0	99	AATGGCTTCACCCCTCTCCATATCGCCTGCAAAAAGAACCGCATCCGAGTAATGGAACTCCTTTTGAAGCACGGTGCATCTATTCAAGCCGTAACCGAG
13	ENSMUSE00001272604	69,877,830	69,877,928	0	0	99	TCGGGCCTTACCCCAATCCATGTTGCTGCCTTCATGGGACATGTAAATATCGTGTCACAGCTAATGCATCATGGAGCCTCCCCAAACACCACCAATGTG
14	ENSMUSE00001220057	69,879,893	69,879,991	0	0	99	AGAGGAGAGACGGCATTGCATATGGCGGCTCGGTCCGGACAAGCAGAAGTGGTGCGGTATCTGGTCCAAGATGGGGCTCAGGTAGAAGCAAAAGCTAAG
15	ENSMUSE00001290652	69,882,361	69,882,558	0	0	198	GATGACCAGACTCCACTCCACATCTCAGCCCGACTTGGGAAAGCTGACATAGTGCAACAACTGTTACAGCAAGGAGCATCCCCCAATGCAGCAACAACTTCTGGG TACACCCCCCTTCACCTTGCGGCCAGAGAGGGGCATGAGGATGTAGCTGCGTTCCTCCTGGATCATGGAGCATCTTTATCCATAACAACAAAG
16	ENSMUSE00001248451	69,884,747	69,884,845	0	0	99	AAGGGATTCACCCCTCTGCACGTGGCAGCCAAATACGGAAAGCTTGAAGTCGCAAGTCTCCTGCTGCAGAAGAGTGCGTCTCCCGATGCCGCAGGGAAG
17	ENSMUSE00001279345	69,885,139	69,885,237	0	0	99	AGCGGGCTAACTCCACTGCATGTAGCAGCGCATTACGATAATCAGAAAGTGGCCCTTCTGCTCTTGGACCAGGGAGCCTCACCCCACGCAGCCGCAAAG
18	ENSMUSE00001278922	69,892,322	69,892,519	0	0	198	AATGGCTATACACCACTGCACATCGCGGCCAAGAAGAACCAGATGGACATAGCCACGTCCCTGCTGGAGTACGGTGCTGATGCAAACGCGGTTACCCGGCAAGGG ATTGCGTCCGTCCATCTTGCGGCACAGGAAGGGCACGTGGACATGGTGTCGCTGCTCCTGAGTAGAAACGCGAATGTCAACCTGAGCAATAAG
19	ENSMUSE00001280782	69,893,445	69,893,543	0	0	99	AGCGGTCTCACCCCACTCCACCTGGCTGCTCAAGAAGACCGAGTGAATGTGGCCGAGGTCCTTGTCAACCAGGGGGCCCATGTGGATGCTCAGACAAAG
20	ENSMUSE00001220119	69,898,041	69,898,139	0	0	99	ATGGGCTACACCCCGCTCCATGTGGGCTGTCACTATGGAAATATCAAAATAGTCAATTTTCTGCTGCAGCATTCTGCAAAAGTTAATGCCAAGACGAAG
21	ENSMUSE00001221633	69,898,228	69,898,326	0	0	99	AATGGATACACAGCACTGCACCAGGCTGCTCAGCAGGGCCACACGCATATCATCAATGTCTTGCTTCAGAACAACGCCTCCCCCAATGAACTCACTGTG
22	ENSMUSE00001248586	69,898,994	69,899,089	0	0	96	AATGGGAACACAGCTCTGGCCATCGCCCGGCGCCTTGGTTACATCTCGGTGGTTGACACACTGAAGGTCGTGACGGAGGAAATTATGACCACCACT
23	ENSMUSE00001261484	69,904,198	69,904,270	0	1	73	ACCATCACGGAGAAGCACAAAATGAATGTCCCAGAAACGATGAATGAAGTCCTCGATATGTCAGACGATGAAG
24	ENSMUSE00001217354	69,904,448	69,904,510	1	1	63	TAAGGAAAGCCAGCGCCCCCGAAAAGCTCAGTGATGGGGAATATATCTCAGACGGTGAAGAAG
25	ENSMUSE00001255465	69,920,438	69,920,491	1	1	54	GTGATAAATGCACATGGTTCAAAATTCCCAAAGTACAGGAGGTTTTGGTGAAAA
1s	ENSMUSE00001275881	69,925,495	69,926,191	-	1	697	GAGAACAAAGTTGAAAGTTTGCCTGCAGCTCCCGGCCACTCCTGCTCCCGGGCCCTTCTTTGTTTTCTCCCTGGGTTTGTTTTTCTTCTACCTGGCTTGGCTGTT TCTTCATTCACTTTTGAGAAGAGCCCGTCTCCAAATCGCCCAGTTACACAAGTGCCCGGGGCTCTCTGGACTTGTGAGGGTCCCTGCTACTCTGACTGCCCTGGT ATCAAGTTACTGAAAGTCTACACCCAGGCAGTCCTCATATTTACATACAAATAACTCCTGGGTTTGCTTTTATGTCACTATTGGGTCCTGCAAGAGGCTTGCCAG AGCGTCCTTAATCCAATCAGGAGGCACTTTGAAAGGATGTCTGTTGAGCGGTCAGAAGGATGTTCGTCGCTATTAAGTGTTGCCACACAAAATTTTTCGCATGTT

							TCGGTCTGAGTTTTTTTTTTTTTTTAAATCTTCGGAGTTAAAAAAGTGAGGAATGATGTACAGCTGCTCAGTTGCCTTCGACAGCTTGGAGATGCTGAGGGAAAC GCTGCAGCCCTGGTGAAGAAGATCTGACTAGGGACGGGTTTGGATCCATACCAGGCTGGTGTGGATTGGGGCTGGTGTGGACGGCTTACTCTAAACCCCTGCTTA AGGAATTCCTGGAAGCCTCGGGAAAGTACTCCCCAACCAGTCGTGGTGGAAATGGCTTTGCCACACA
26	ENSMUSE00001309139	69,927,695	69,927,818	1	2	124	GTGAAGATGCCATCACAGGGGACACTGACAAGTATCTCGGGCCACAGGACCTTAAGGAGCTAGGTGATGACTCCCTGCCAGCAGAAGGTTACGTAGGCTTCAGTC TTGGAGCCCGTTCTGCCAG
27	ENSMUSE00001230155	69,929,447	69,929,458	2	2	12	TCCCAAGATAAG
28	ENSMUSE00001286314	69,932,394	69,932,496	2	0	103	CCTCCGCTCCTTCAGTTCGGATAGGTCCTACACCTTGAACAGAAGCTCCTACGCAAGGGACAGCATGATGATAGAGGAACTTCTGGTACCATCCAAAGAGCAG
29	ENSMUSE00001255995	69,950,952	69,951,058	0	2	107	CACCTGACGTTCACGAGGGAGTTTGATTCTGACTCCCTCAGACACTACAGTTGGGCAGCGGACACGTTAGATAATGTGAACCTGGTCTCAAGCCCGGTGCATTCT GG
30	ENSMUSE00001220072	69,953,440	69,953,472	2	2	33	CTGCTCGTCTCCGCTGCCTCAGTATGACTCAAG
31	ENSMUSE00001208972	69,955,926	69,956,150	2	2	225	GTTTCTGGTTAGCTTTATGGTGGACGCGAGAGGGGGCTCCATGCGAGGAAGCCGCCACCACGGGATGCGGATCATCATCCCTCCGCGAAAGTGTACGGCCCCCAC CCGCATCACGTGCCGCCTGGTAAAGAGACATAAACTGGCCAACCCACCCCCCATGGTGGAAGGAGAGGGATTAGCCAGTAGGCTGGTAGAAATGGGTCCTGCGGG GGCACAATTTTTAGG
32	ENSMUSE00001230547	69,958,918	69,959,072	2	1	155	CCCCGTCATTGTGGAAATCCCTCATTTTGGGTCCATGAGGGGGAAGGAGAGAGAACTTATCGTCCTTCGGAGCGAGAACGGAGAGACCTGGAAGGAACATCAGTT TGACAGTAAAAACGAAGACCTCGCGGAGCTTCTCAATGGCATGGATGAAG
33	ENSMUSE00001292195	69,973,722	69,973,933	1	0	212	AACTCGACAGCCCGGAAGAGTTGGGTACAAAGCGCATCTGCAGAATTATCACAAAGGATTTCCCCCAGTATTTTGCCGTGGTTTCCCGGATTAAGCAGGAAAGCA ACCAGATCGGTCCTGAGGGTGGGATTCTGAGCAGCACCACCGTGCCCCTCGTCCAGGCCTCCTTCCCAGAGGGCGCCTTAACCAAGAGGATCCGTGTGGGTCTCC AG
34	ENSMUSE00001268073	69,976,048	69,976,255	0	1	208	GCTCAGCCCGTGCCAGAGGAAACGGTAAAAAAAATCCTTGGGAACAAAGCAACATTTAGCCCAATTGTCACGGTAGAGCCGAGGAGAAGGAAGTTCCATAAGCCG ATCACCATGACCATTCCGGTGCCCCCGCCCTCGGGAGAAGGCGTGTCCAATGGGTACAAGGGGGATGCCACGCCCAACCTGCGGCTCCTCTGCAGCATCACAG
35	ENSMUSE00001205997	69,977,713	69,977,809	1	2	97	GAGGCACCTCACCAGCTCAATGGGAAGACATCACAGGAACAACCCCTCTGACGTTCATAAAGGATTGTGTGTCTTTCACAACCAACGTTTCAGCCAG
36	ENSMUSE00001252247	69,978,471	69,978,699	2	0	229	ATTCTGGCTGGCGGACTGCCATCAGGTGTTAGAGACCGTAGGGCTAGCCTCCCAGCTGTACAGAGAGCTGATATGCGTTCCCTACATGGCCAAGTTCGTTGTGTT TGCCAAAACAAACGACCCGGTGGAGTCCTCGCTGAGGTGCTTCTGTATGACAGACGACAGGGTGGACAAAACCCTGGAGCAGCAGGAGAACTTCGAGGAGGTTGC CAGAAGCAAAGACATTGAG
37	ENSMUSE00001292473	69,979,318	69,979,443	0	0	126	GTTCTGGAAGGAAAGCCCATCTACGTTGATTGCTATGGAAACCTGGCCCCTCTGACCAAAGGAGGACAGCAGCTTGTTTTTAACTTTTATTCTTTCAAAGAAAAC AGACTGCCATTTTCCATCAAG
38	ENSMUSE00001279827	69,980,272	69,980,394	0	0	123	ATCAGAGACACCAGTCAAGAGCCCTGTGGCCGCCTGTCTTTCCTGAAGGAGCCAAAGACAACAAAGGGATTACCCCAAACAGCTGTTTGCAACTTAAATATTACT CTGCCGGCACATAAAAAG
39	ENSMUSE00001209441	69,980,824	69,980,850	0	0	27	GAGACAGAGTCAGATCAAGATGATGAG
40 40s	ENSMUSE00001278273 ENSMUSE00001236257	69,982,116	69,982,197 69,982,161	0	1	82 46	GCTGAGAAGGCAGACAGACGCCAGAGCTTTGCCTCCCTAGCTTTACGTAAGCGCTACAGCTACTTGACTGAACCCAGCATGA
41L 41S	n/a ENSMUSE00001253692	69,986,083	69,993,762 69,988,632	1	1	7680 2550	AAACAGTTGAACGGAGTTCAGGAACAGCAAGATCCCTCCCCACCACTTATTCACACAAGCCATTCTTTTCTACAAGACCATACCAGTCCTGGACCACGGCTCCAA TCACAGTGCCCGGGCCGGCCAAGTCAGGCTCCTTATCCAGCTCTCCCTCTAACACGCCGTCAGCTTCTCCGTTAAAATCCATATGGTCTGTCTCGACGCCTTCTC CGATCAAATCCACGTTAGGCGCCTCAACTACATCTTCAGTCAAATCCATTAGCGACGTGGCGTCTCCTATTAGATCTTTCCGGACAGTTTCTTCGCCAATAAAAA CGGTGGTGTCGCCGTCTCCGTACAATCCCCAGGTTGCCTCTGGTACCCTTGGGAGGGTTCCCACCATCACAGAGGCCACACCCATAAAGGGGCTGGCTCCCAACT CAACTTTCTCCTCTCGAACTTCTCCTGTGACGACCGCAGGGTCTCTGTTGGAGAGGTCCTCCATCACCATGACACCCCCTGCCTCCCCCAAATCAAACATCACTA TGTATTCCTCAAGCTTGCCATTTAAGTCCATTATCACATCAGCGACACCACTGATCTCTTCCCCTTTAAAGTCAGTGGTGTCTCCGACCAAGTCTGCAGCTGATG TCATCTCAACAGCTAAAGCTACGATGGCATCGTCTCTCTCCTCCCCCTTAAAGCAGATGTCCGGACATGCAGAGGTAGCGCTAGTCAATGGGTCTGTTTCTCCTC TGAAGTACCCTTCGTCTTCAGCTTTAATTAACGGATGCAAAGCCACTGCCACATTACAGGACAAAATTTCTACAGCCACAAACGCTGTGAGCTCGGTGGTGAGCG CAGCCTCTGACACGGTGGAGAAAGCGCTCTCTACCACGACAGCCATGCCCTTTTCCCCACTCAGGTCGTATGTTTCTGCAGCCCCCTCGGCTTTCCAGTCCCTTA GAACTCCCTCTGCAAGTGCACTGTACACCTCCCTCGGGTCCTCGATAGCTGCTACTACCTCATCTGTAACTTCATCAATAATCACAGTGCCAGTATACTCGGTAG TCAATGTTTTGCCAGAACCAGCACTGAAGAAACTCCCAGACTCTAACTCGTTCACCAAGTCGGCAGCGGCTTTGCTGTCGCCCATTAAAACATTGACTACGGAGA CACGCCCTCAGCCCCATTTCAATCGAACTTCATCTCCAGTCAAGTCGTCTCTGTTCCTGGCGTCCTCGGCCCTTAAGCCATCAGTACCATCTTCTTTATCTTCCA GCCAGGAGATCTTAAAGGATGTGGCCGAGATGAAGGAAGATCTCATGAGGATGACTGCCATACTGCAGACAGACGTGCCTGAGGAGAAGCCATTCCAAACCGACC TCCCCAGAGAAGGGAGAATAGACGATGAAGAACCTTTCAAAATCGTTGAGAAAGTGAAGGAAGACTTAGTCAAAGTCAGTGAGATACTCAAAAAGGACGTGTGTG TCGAGAGCAAAGGGCCACCCAAGTCCCCGAAGAGTGACAAAGGACACTCTCCAGAGGATGACTGGACAGAATTTAGTTCTGAGGAAATACGAGAAGCCAGGCAGG CTGCGGCCAGTCACGCCCCGTCCCTGCCTGAGAGAGTACACGGGAAGGCCAACCTCACTAGAGTCATAGACTACCTGACCAATGACATCGGGAGCAGCTCACTGA CCAACTTAAAGTACAAGTTTGAAGAGGCTAAGAAGGATGGAGAGGAGAGACAGAAGAGGATTTTAAAGCCAGCCATGGCCTTGCAGGAGCATAAACTCAAAATGC CGCCGGCCTCCATGAGGCCTTCCACCTCTGAGAAGGAACTGTGCAAGATGGCTGACTCTTTTTTTGGAGCAGATGCCATCCTAGAGTCTCCCGATGACTTTTCCC AGCATGACCAAGATAAAAGTCCCTTGTCTGACAGTGGCTTTGAAACCCGCAGTGAGAAAACACCTTCGGCCCCGCAAAGTGCCGAGAGCACAGGCCCTAAGCCGT TATTTCACGAAGTCCCCATCCCCCCTGTCATCACAGAGACAAGAACTGAAGTGGTCCATGTGATCAGGAGCTATGAGCCCTCTTCTGGAGAGATCCCCCAGTCCC AGCCAGAGGACCCCGTGTCTCCCAAGCCTTCCCCTACTTTTATGGAGTTGGAACCAAAACCCACCACCTCTAGCATCAAGGAAAAAGTAAAAGCATTTCAGATGA AAGCCAGTAGTGAGGAAGAGGACCACAGTCGGGTTCTAAGCAAAGGCATGCGTGTCAAAGAAGAGACTCACATCACCACGACCACCAGGATGGTGTATCACTCCC CTCCTGGTGGCGAGTGCGCCTCCGAAAGGATTGAGGAGACCATGTCAGTCCATGACATCATGAAGGCCTTTCAGTCCGGGCGAGACCCTTCCAAAGAGCTGGCAG GGCTGTTTGAACACAAGTCGGCCATGTCTCCAGATGTTGCCAAGTCTGCTGCTGAGACCTCAGCCCAGCACGCAGAGAAGGACAGCCAAATGAAACCCAAACTGG AGCGCATTATAGAAGTGCACATCGAAAAAGGTAACCAAGCCGAACCCACTGAAGTCATTATTAGAGAGACCAAAAAGCATCCCGAGAAGGAAGTGTCTGTGTATC AGAAAGACTTATCCCGGGGAAATATTAACTTAAGAGATTTTCTGCCAGAGAAACACGATGCTTTCCCCTGCCCCGAGGAGCAGGGTCAGCAAGAAGAAGAAGAGC TGGCAGCCGAAGAGTCCTTGCCTTCTTATCTGGAATCCTCCAGAGTAAACACTCCAGGGTCCCAAGAAGAAGATAGCCGCCCTAGTTCCGCACAGCTCCTGTCCG ATGACTCTTATAAAACACTGAAGCTTTTGAGTCAGCACTCCGTAGAGTATCATGACGATGAGTTGTCAGACCTAAGAGGGGAGTCTTACAGGTTTGCTGAGAAAA TGCTTCTCTCAGAAAAGCTAGATGTGTCTCACTCTGATACCGAGGAGTCGGTGACAGACCATGCAGGACCCCCTAGCTCAGAGTTACAGGGGTCTGATAAGCGAT

							CCAGAGAAAAAGTAGCCACTGCCCCCCCAAAAGAAATCCTCTCCAAAATCTATAAAGATGTATCTGAAAATGGGCTAGGGAGAGTGTCTAAAGATGAGCATTTTG AGAAACTGACAGTGTTGCACTACTCGGGCAATGTCAGTGGTCCCAAGCATGCCATGTGGATGCATTTGTCTGAGGACAGACTAGACAGAGGTAGAGAGAAGCTGA TGTATGAAGATAGGGTGGACAGGACCGTGAAGGAGGCGGAAGAGAAGTTGACTGAAGTGTCGCAGTTTTTTCGTGACAAAACTGAGAAGCTAAACGATGAACTGC AGTCCCCGGAGAAAAAGCCACGCCCCAAAAACGGCAAGGATTACTCCTCCCAGAGTTCCACCAGCAGTAGCCCCGAGAAAGTGTTAACGGAGCTGTTGGCATCCA ACGATGAATGGGTTAAGGCCAGGCAGCGTGGCCCGGATGGACAAAGTGTCCCTCAGGCTGAGGACAGGAAGGCACCCAGTAGGTCCAACAGCCCTGAGAACAGGG TCCCTACCCAACAGAGCGAGGATGACCAGCCTCCAGAGGAAGCCAAAAGAACTGTCGTTGCTCAGAGCAGGGGACAAGAAGGACCCCAGTCTGGATTTCAGCTCA AACAATCGAAACTCAGTTCCATTAGATTAAAATTCGAACAAGGGGCACGTGCCAAAAGTAAGGATCCACCTCACGAGGAGAAACATCTGGACGGGCCGTCCCGAA TCCCGGTTAAGAAAACTCAAGAAACCAAACTGCCCACGCACCCAGGTTTTGCTAGAGAAAAACAGCAGAAGGCTGTAGATCCCCTAGAGGAAAGAGTGCCAGTGC AAAATGATGTTACGGTATTCAAAGCCGACCATGCCCAAAGCAATGAGATCGTTACAAGCAAATCTGGCTCCGGCAATGGCAAAAGCCACAGAACTGAGATGTTAA GTAAGGCAATGCCTGACTTCTTTCCTGAGCAACAGGTTGAAGACTCAGCCTGCCCCATAACATCAGATCTAGAGACCAAGGGACCGTGGGACAGAAAGGTCTTTA GAACATGGGAAAGTTCTGGGGCCAATAACACTAAGGCCCAGAAAGAGCAACTCTCCCATGTGCTCGTTCACGATATAAGAGAGAATCACGCTGGTCGCCCTGACG ATAGTGAGAACGGTGACCCAAAGAGTGGATTTATGTATGTGACTGAGAGAGAACACAAAATGTTAACGAACGGCTCTCTCTCAGAAATTAAGGAAATGAGTGTAA AATCTCCCTCCAAGAAAGTGTTATACAGGGAGTACATTGTTAAAGACGGGGACCCTCCCAGCAGCGCTCTCAACCATCCCCCCAGGAGAAGTGAGAGCTCGCTAG CATCTCACATTCCCATCAGGGTCACAGACGAGAGGAGGATGCTGTCGTCAAACATCCCCGATGGGTTTTGTGAGCAGTCAACATTTCCAAAACAAGAACTATCCC CAAGAGTGTCCCGGCCAAGTATGAGCGAAGGGGTAGTTGAGAGCCAGCACTTTAACTCCGTAGACGATGAAAAAGTTACCTATTCCGAGATCAGCAAAGTTTCCA AACATCAGAGTTACCTAGCTCTTGATGAAACCGAGACCTCTCCCACCAAATCTCCCGACTCATTAGAGTTTAGCCCAGGGAAGGACTCTCCCTCTAGTGATGTGT TCGACCACGGTTCCGTGGATGGGTTGGAGAAGACAGAGGGGGGGAAAGAGATCAAAACCTTACCTGTCTATGTCAGCTTCGTGCAAGTGGGGAAACAGTACGAAA AGGAGCTCCAACCAGGAGGTGTAAAAAAGATCATCAGTCAGGAGTGTAAGACGGTGCAGGAAGCCAGGGGGACCTTCTATACAGCTAGACAGCAAAAGCAGCCTC CGTCTCCCCAGGGCAGTCCAGAAGATGATACTCTAGAGCAAGTGTCCTTTCTAGACAGCTCTGGGAAGAGCCCTTTGACCCCGGAAACTCCCAGTTCAGAGGAAG TGAGTTACGAGTTCACATCTAAGACACCAGACTCACTCATAGCTTTTATACCAGGACAACCCAGCCCGATTCCCGAGGTTTCAGAGGAGTCGGAGGAGGAGGAGC CCAAATCAGCCCCACTAAGGCAGGTGACCGTGGAGAAGGAAACAGATCGTGACGTGAGCAAAGACTCTATCCAAAGACCCAAATGTAACCGAGTTGCCTATATTG AGTTTCCCCCTCCTCCCCCGCTGGATGCTGACCAGATGGAATCAGATAAGAAACATCAATATCTCCCCGAAAGGGAGGTTGACATGATGGAGGTCAGCCTTCAGG ACGAGTCTGACAAGTACCAGTTGGCCGAGCCAGTCATCCGAGTGCAACCCCCATCACCAGTCCCTCCCGGTGCCGAGGCCAGTGACTCCAGCGATGATGAGTCCT TGTACCAACCAGTCCCAGTTAAAAAATACACCTTCAAGTTGAAGGAAGTTGACGAAGGGCAGAAAGACACGGCGAAGTCCAAAACCGCCGCCACAAAAGCTTCCA ACCAGAAAGAGGCAGATGGTAACGGGAGAGAGGGCGAATCTGGCCTTGACTCCCCTCAGAACGAAACAGCTCAAAATGGAAACAATGACCAGTCTGTCACAGAGT GTTCCATTGCGACCACGGCTGAGTTTTCTCATGACACAGATGCCACGGAGATAGACTCTCTGGATGGCTATGACCTACAGGATGAGGATGACGGTCTAACAGAGA GCGACTCTAAACTCCCAAGTCAGACCATAGACACCAAGAAGGATGTTTGGACGGAGGGCATTCTGAAGCCGGCTGACCGCTCTTTCAGTCAGAGCAAACTGGAAG TTATTGAGGAGGAGGAGGGGAAAGTGGGGCTGGACGAAGAGAAACCATCACCTTCTAAAAGCCCATCATCCGACAGAACCCCAGAGAAGGCCGATCCCAAGTCAG GGGCCCAGTTTTTCACCCTGGAAGGCAGACACCCGGACAGATCAGTGCTCCCTGATACTTACTTCAGTTACAAAGTTGACGAAGAATTCGCCACTCCTTTTAAAA CAGTGGCGACCAAAGGTCTCGACTTTGACCCTTGGCCCAATAACCGAGGGGACAATGAAGTTTTTGACGGTAAATCTCGGGAAGATGACACTAAGCCATTTGGTC TGGCGGTGGACGACCGCTCGCCGGCAACCACCCCTGACACAACGCCAGCCAGAACACCAACTGACGAAAGTACCCCAACTAGTGAGCCTAACCCCTTCCCATTTC ATGAAGGAAAAATGTTTGAGATGACTCGCAGTGGTGCAATTGACATGAGCAAGAGAGATTTTGTGGAAGAGAGGCTCCAATTTTTCCAGATTGGTGAGCATACTC CTGAAGGGAAGTCAGGGGCCCAGGGGGAAGGGGATATGGTCACTGATACCCCACAGCCACAGTCAGGGGACACCTCGGTAGACACCAATCTAGAGAGAGATGTAG TGGCACCTTCAGTCGACCCCAACCCCAGCATCCCGAGCAACGGAGAGTGTCAGGAAGGCACAGCCTGTAGTGGCTCTCTGGAGAAGTCGGCAGCTGCCACTAACA CCTCAAAAGTTGACCCCAAGTCACGCACGCCTATAAAAATGGGAATTTCTGCATCTACCATGACCATGAAGAAAGAAGGCTCTGGAGAAGTGACAGATAAGACAG AGGCTGTGGTGACCAGTTGTCAGGGGTTAGAAAACGAAATCGTGAAAGAGATCTCGAGTGCACCCAGTAGCCAGGTGGGCATTAGGCCCCAAGAGAAACACGATT TTCAAAAAGATAACTTTAATAACAACAATAATCTGGATGCTTCCACTATGCAGACAGATAACAGCACAAGCCACATAGTTCTGACAGGACGCGCTGCATCCACTT GCACCACAGAGGAAGCTAATCCAGTAAAAGGCTCAGGAAAGAGTCCAGGGACTCAAGGACACTCCAGCAGAGAGTCTCGGAAGGAGCCGATAGGGCTTAGGCGGA AATCCAAGCTTCCTATAAAGGCCACCGCACCAAAAGATGTCTTCCCGCCAAACCATAAGGCAGACAGTAAAACAGGTAAACCGAGGCAGGTTGGTCAATATGAGA AACACAAAGCCCTTCCTACTTCTTCATGTTTAGATGCCAAGTCCCGAATTCCCGTCAAAAACACACACAGGGAGAACCTAGTTTCAGTCAGAAAAGCATGCGCCA CACAAAAGCGAGGGCAGCCAGAGAGAGGCAAGGCCAAACAGCCTCCATCCAAGTTGCCAGTAAAGGTAAGATCCACCCGTGTCACCGTCACCACCACCAACACCT CCACCACCACTACCACCACCACCACCACCACTACCACCACTACCGTTAAAGTTACAGAAAGTCAGCTTAAGGAGGTATGTAAACATCCCATTGAATATTTTAAGG GAATTAGTGGCGAGACCCTAAAACTTGTGGACCGCCTCACTGAAGAAGACAAAAAGATGCAATCGGAGTTGTCTGATGAGGAAGAAAGTACCTCAAGGAACACGT CGTTGTCCGAGACTTCCCGGGGCGGCCAGCCTTCAGTTACCACGAAGTCTGCTAGAAATAAGAAAACAGAGGCACCGCCCTTAAAATCAAAGAGAGGAAAGGCCG GCAGTAGGAGGACTG
42	ENSMUSE00001231047	69,994,372	69,994,446	1	1	75	GTCCGCAGAGTCCTTGTGAGCGGACGGATATCAGGATGGCGATAGTAGCCGATCACCTGGGACTTAGTTGGACAG
43	ENSMUSE00001259541	69,998,095	69,998,226	1	1	132	AGCTGGCAAGGGAACTGAATTTTTCAGTGGATGAAATCAACCAAATACGTGTGGAAAATCCCAATTCTTTAATTTCTCAGAGCTTCATGTTATTAAAAAAGTGGG TGACCAGAGACGGAAAGAATGCCACAA
44	ENSMUSE00001257460	69,999,355	69,999,498	1	1	144	CTGATGCCTTAACTTCGGTCTTAACGAAGATTAACCGGATAGACATTGTAACTCTGCTGGAAGGACCAATATTTGATTATGGGAATATTTCAGGCACCAGAAGCT TTGCAGATGAAAACAATGTTTTCCATGACCCAGTTGATG
45l 45a 45	ENSMUSE00000642788 ENSMUSE00001239902 ENSMUSE00001282241	70,001,923 70,002,511	70,002,601 70,002,231	1 1 1	2 1 2	679 309 91	GTCACCCTTCCTTTCAAGTGGAGCTGGAGACCCCCATGGGGTTGTACTGCACACCACCCAACCCTTTCCAGCAAGATGACCATTTTAGTGATATCTCTAGCATAG AGTCTCCCTTTAGGACCCCCAGTAGACTGAGTGACGGGCTGGTGCCTTCCCAGGGAAACATAGAGCATCCAACAGGTGGACCTCCAGTGGTAACCGCAGAGGACA CTTCTTTAGAAGACAGCAAAATGGACGATTCTGTAACTGTAACAGACCCGGCCGACCCACTGGACGTAGATGAGAGCCAGTTGAAGGACCTGTGTCAGAGCGAGT GTGCTCAGTGCTGGGCGAGTGTGCCCGGGATCCCAAACGACGGTCGGCAGGCAGAGCCACTGAGACCGCAGACTAGAAAAGTAGGCATGAGCTCTGAACAGCAGG AAAAAGGAAAATCTGGTCCTGATGAGGAAGTGACAGAAGACAAGGTCAAATCTCTGTTTGAGGACATTCAACTTGAAGAAGTAGAGGCTGAGGAGATGACAGAAG ACCAGGGGCAGGCTATGCTTAACCGTGTTCAGCGAGCAGAACTGGCAATGTCTTCACTTGCAGGTTGGCAGAACGAGACGCCAAGTGGAAGCCTAGAGTCCCCAG CGCAAGCTCGAAGACTAACTGGTGGGTTACTGGACCGTCTGGATGACAG
46	ENSMUSE00001280544	70,004,610	70,004,991	2	0	382	CTCTGACCAGGCTCGGGATTCTATTACCTCATACCTCACGGGAGAACCTGGGAAGATCGAAGCAAATGGAAACCACACAGCGGAAGTCATTCCAGAAGCAAAGGC AAAACCCTACTTCCCGGAATCCCAAAACGATATAGGGAAACAGAGCATCAAGGAGAACCTGAAACCAAAAACACACGGATGTGGTCGCACTGAGGAACCAGTGTC GCCCCTCACAGCCTACCAGAAATCTCTGGAAGAAACCAGCAAGCTTGTCATAGAAGACGCACCTAAACCCTGTGTGCCTGTCGGCATGAAAAAGATGACCAGGAC TACGGCTGACGGCAAAGCCAGGCTCAACCTCCAGGAAGAAGAGGGGTCCACCAGGTCAGAGCCTAAG
47	ENSMUSE00001243294	70,006,803	70,006,853	0	0	51	GTCAAAAGCCCGGGCGAAGCGTTTACGCGGATGACCGCCTGCTGTTACAAG

48	ENSMUSE00001310630	70,008,778	70,008,864	0	0	87	GACTTGAGAAACAGTGAGAGTGATTCAAGCTCAGAGGAGGAGCAGAGGATCACTACCCGGGTCATACGAAGGCGTGTGATTATAAAG
49	ENSMUSE00001226504	70,013,972	70,014,055	0	0	84	GGGGAGGAAGCCAAAAACATCCCTGGTGAATCTGTCACAGAAGAGCAATTTACTGATGAAGAAGGCAACCTCATCACGAGAAAA
50	ENSMUSE00001227898	70,014,190	70,014,246	0	0	57	ATCACTCGGAAAGTAATAAGACGGATTGGTCCACAAGAGAGGAAGCAGGATGACGTG
51	ENSMUSE00001313132	70,015,568	70,015,653	0	-	86	CAGGGAGAAGGCTATAAGGTGAAGACGAAGAAGGAAATCCGGAACGTGGAGAAGAAAACCCACTAGTGACAGTGACGTCAGTCCAG
52	ENSMUSE00000612179	70,023,832	70,027,438	-	-	3607	GACCACTTGGTCATACTGCCAGTATTGAGAAACTCACCAGAGATCAGCAGGAAGAAAAATAGTCACCAAGAGTGGAGTGTGGGTCAGCTGCTTCCACCACACGTC AGTGACACGATTTTTTTTTGTAAACGCAGAAGGAAAACGAAAATCACATTTTTTCTTTCATTTAGCATGAGCCGATCTACAAAGCATGGAAACTCACATTCATT CCCGGCACTGAAATGCACACTGAGCAAGTGCAGTGTACGACACAGGAAGCCATGTTCTTCAGACCCGGTCTCAAGTAATTTAGTGTCATTTTCAAAGAAGACAGA CAAAACAACACCTGTGCCACCCAGGAGGAGGGGCAGCAGAGGACGGAATGATCAAATCAAGAAGACACACTAAAATTACTAAATTCACAACAGCTCGCCTTATTT TTCTCGGACCCAAACTAACTGTCAGGGTATAAACACTGTTCCTTTCTTTCTTTCTTTCTTTCTTTTTTTTTTTTAAAGAAAAATAATAATAATAATAATGAA AAAAATCAATAGTTTTGCTGTAAATAATAACACTGTAAATTCTAACAGAAGAAACTACAATAAAGAATTATAAGGCACCCGCCTCACAGAACACAAAGATATCAC AAATGCATCCAAGGACAGGCGTCCCAAGTGACTTCACCCTGGACAAGGATGGGGATCCAGCGCTCTCGGGACTCTTTCACTGACTCTTGTATATTAGCAATTATG TTTGTACACGCAAAACTGCTAGCTTGATTTTAAAAGAAAAAAAATGCAAATCTTTAAAAAGGAAAAAAAAAAAAAAACCTGCTGCAAATTTAAATAATTCCCCAA ACGAGGAATTCTGTAGTTCTGTGAAAAAAAATTTTTTTTTCTTCAGAATATTAATATTTTGATGCATGCATATCACCTTATTTTGATTAAATCTTTTCCAATTTT GCAAACACTACAGTCTCCTGCAACATGGGAGATTTTATCTGTAAACACAAAGCCCTTCATCTAATATTTATTGCTATTGCCAATTTTTCAATGAAATGACCAAAA ATGGAAAAAAAAAATAACTATACAGTAGTTTGCTTGGGGGTGGGGGGAGGGGCGCTGTTAGTGCTTACAGGGGGGAAATGCTTGCCACTGTAGAAGTGGATGGTGC TCACAAGAGGCCCCAGTCGTGGGTATTTAAAAAAATGGACTGACCGGAAATCCGTATCTAGCAGGATCGAAGCGCACTGTAAAAAAAAAAAAAAAGACAAAAAAA AAAAAAAAAAAGATCGCTGTATTGTGTACTGGCTCTGAGATGTAGACCCCTTTCAGCAAGCCAATCACTAGTAACCATCCCAGCAGTGCCCCCATTAGGTTAGCG GGGCTGCCGCGTTTTATAGAGCATTTTTCTTTGGGTTTGGTGAGGTTCCTTCATTCACTATCTTAACTTGAAATCGACCTCCACGGACACCTAGCTCTAAATGAC ATGTATGAGAAAAGCAGACGCCGGATAAGCTAGTCGATTATTTAAGCATATAAAATAAACTGTGTTCAACTCTTCACCTACTTGGGTTCCACAGTGTTCTTGTAT CCTCTGGCAAAACCTAGCTGTCTAATCCCCAGTCACAGGGGCCCTGTCTGTGCCTCCAGTCACTAAAGCCATACTCTGGAACGTTCTGCTCTCTCCCGAAAACAC CCACCTTGCATAAACTCTGTGCACTTTGTGGGGGAGCTAAGAATTTAAAGATGAAGTAATCTTCGTCTATTTAGGCTCTTCTGCCCCATAGAAGAAGATGGGATT TATAAGGCCAGTGTGTCAAGAAGTTATGCTGTTCCCAGGGAGCATCTATCTGTGGTTGATTTTTTTTTTTTTTTTTACCCCCCAGGAAGCATTGGTTTAGGTTTT GTGTCATTAGTTTGCGGGCTTGGAGATTTTGTCATCACTGTTCTTGAGACAAGGTCTCAAAATGTCTGCTTAGTTTCTTAACTGATATGTTGTCAGAGCTTACAG ATTGAGAAATTTTGCTAATAACTCGAGATTTTTTTATTTTACCAGTTTATTTTGGTACTGGTCATCATGCATGCTAAAAGATGTGAACTACCACTAAGCAGCACC CTCGGCCTTCCCTGGATATTTCTGAGACGGCCTCACTAGCTGGTCCAAGCTGGCCTTGACTTTCCGAGGCTTCTGCCCTGTTTACTTAAGAGGGCTGCGCCACCA GACTGAACAGGGGTTCTCTTGTGAAGCAACCTCCGGCAACAGCAGACCGCCCACTCCAAAAGACGTTGTAGGTGTGACCCCTACTCTCTCCAGCTACATTTGTGA TCCCCGTCATCCTAGCCTTATTTCCTACCTAACCCTGAGAGGCACTTGGAGTTTGGGGCCCACTGATTTCATAACTCAAAGAGTTCAAAGATCTCATGCCTTTGA TTCAACTTTTACCCCGGCCCACAGCCAGGCATGGCACATTAGGGGTGGTATCTCTCACCATCCTAAACTTCAAGTCCACACTATAACATTTTTCTTCTAAATACA TTCCATTCATTGACTCGGTCCTTACCACCACTGTGTGAGTTAGATACTATCTTTGATGTAACAGGCCCCATATAGTATTAATGAATGCTTAATGTCATTCAAGGC TGTTATTGCCTGTCCTATGGGATGAATATTCTCCAGAATTCCAGCCAGAAGACAAGTACCAGAGAGCCTATTTGGTCTAGAGAAGCCGCTTTCAATAAACAAAGA GGCAGAGAGTACATTTGCATGTCATTTGCATGATGTCTGTGTCTACACCCCCAACCCCTGCCAATCAGAAACATCTAAACGACAAGCTGCCACACCTGAAAGTTT TTTTAAAAGTCCCCAAAGCTTCTACATAACTAATAACAGAATATAAGAATGTTAACATCTCATTTAAGAGCTATGAATTCCAGACCCTCTGGCGTTGCTAGAGAT TATTCAGATTTAGAAACTTAATGGGGTTATGTTACATGCCTGGAAATGTGACTTCAGGAACAGGTTGAGAGGTTCAGATGACACCAAAGCCATGAGTTGACCCAG AAGTCTCTGAAGTACGATAGATTTTATTTACGCCTCTAACTTCTGTATATACTGCACCGAAATGGGACATAATGTTTGTATTTCCCTGTCAGCTCACTTAAATGT ATTAAGATTTTTCTTTGACATTTTTGTAAAGAGAGAGAGAGAGAGAGAAAGAAAGAAAGAACTGTGACTGATAAAATCCTGAGATTTGCCACTTCTCCTTTATAC ATTTTTACCCATTTGTTAACATGAAAGGGTTGTTTCTAGAAGGGACTCTCTTCACTGGCCACTCAAGCAACAGAGCTGGCTCTCTCACACTGGTATCCCAGCATC CCACCATGTTCTTCTTAGCCGTCACCTTGGGGCTCCATACAATGGAAGTTTCTCTCCATGGTTAATAAACGTCGATGGAAAAGTGGTTTGCTTGACTTTCTTCAA AGCCTCCCGCTCACATTTGACCGTGAGGAGCCCAGAAAGAAGCCACAGGAACAGCAACTATAGAACTTCGTGCCTCATCCAGGGGCATCTGGGTATTTGTTGGCC AGGCAACTGGCATATTAAAAGGTGTATCATTTCCTAA